2962–2979 *Nucleic Acids Research, 2005, Vol. 33, No. 9*
doi:10.1093/nar/gki603

The ELAV RNA-stability factor HuR binds the 5′-untranslated region of the human IGF-IR transcript and differentially represses cap-dependent and IRES-mediated translation

Zheng Meng[1], Peter H. King[2,5], L. Burt Nabors[2], Nateka L. Jackson[3], Ching-Yi Chen[1], Peter D. Emanuel[1,3,4] and Scott W. Blume[1,3,4,*]

[1]Department of Biochemistry and Molecular Genetics, [2]Department of Neurology and [3]Department of Medicine and [4]Comprehensive Cancer Center, University of Alabama at Birmingham, Birmingham, AL, USA and [5]Birmingham Veterans Affairs Medical Center, Birmingham, AL 35294, USA

Received March 24, 2005; Revised May 2, 2005; Accepted May 2, 2005

ABSTRACT

The type I insulin-like growth factor receptor (IGF-IR) is an integral component in the control of cell proliferation, differentiation and apoptosis. The IGF-IR mRNA contains an extraordinarily long (1038 nt) 5′-untranslated region (5′-UTR), and we have characterized a diverse series of proteins interacting with this RNA sequence which may provide for intricate regulation of IGF-IR gene expression at the translational level. Here, we report the purification and identification of one of these IGF-IR 5′-UTR-binding proteins as HuR, using a novel RNA crosslinking/RNase elution strategy. Because HuR has been predominantly characterized as a 3′-UTR-binding protein, enhancing mRNA stability and generally increasing gene expression, we sought to determine whether HuR might serve a different function in the context of its binding the IGF-IR 5′-UTR. We found that HuR consistently repressed translation initiation through the IGF-IR 5′-UTR. The inhibition of translation by HuR was concentration dependent, and could be reversed *in trans* by addition of a fragment of the IGF-IR 5′-UTR containing the HuR binding sites as a specific competitor, or abrogated by deletion of the third RNA recognition motif of HuR. We determined that HuR repressed translation initiation through the IGF-IR 5′-UTR in cells as well, and that siRNA knockdown of HuR markedly increased IGF-IR protein levels. Interestingly, we also found that HuR potently inhibited IGF-IR translation mediated through internal ribosome entry. Kinetic assays were performed to investigate the mechanism of translation repression by HuR and the dynamic interplay between HuR and the translation apparatus. We found that HuR, occupying a cap-distal position, significantly delayed translation initiation mediated by cap-dependent scanning, but was eventually displaced from its binding site, directly or indirectly, as a consequence of ribosomal scanning. However, HuR perpetually blocked the activity of the IGF-IR IRES, apparently arresting the IRES-associated translation preinitiation complex in an inactive state. This function of HuR as a 5′-UTR-binding protein and dual-purpose translation repressor may be critical for the precise regulation of IGF-IR expression essential to normal cellular homeostasis.

INTRODUCTION

The type I insulin-like growth factor receptor (IGF-IR) is expressed on the surface of essentially all proliferating cells, where it mediates the autocrine and paracrine activities of IGF-I and IGF-II (1,2). Signaling through the IGF-IR is critical to the physiological regulation of cell proliferation, differentiation and survival (3–5), and may also be central to the regulation of mammalian lifespan (6). However, IGF-IR has also been shown to facilitate establishment and maintenance of the transformed phenotype (7,8), and to exert a potent anti-apoptotic effect (9–11), which may contribute to

*To whom correspondence should be addressed at 1824 6th Avenue South, Wallace Tumor Institute, Room 508, University of Alabama at Birmingham, Birmingham, AL 35294, USA. Tel: +1 205 975 2409; Fax: +1 205 975 6911; Email: scott.blume@ccc.uab.edu

the molecular pathogenesis of tumors in which IGF-IR is overexpressed (12,13). Therefore, precise regulation of IGF-IR expression is crucial for maintenance of normal cellular homeostasis, and this may require that IGF-IR expression be regulated at multiple levels.

A series of extensive investigations have established the importance of transcriptional regulation for the control of IGF-IR expression (14–17). As an example, wild-type p53 has been shown to suppress IGF-IR promoter activity, while mutant p53 has been found to up-regulate IGF-IR mRNA synthesis (18). However, several lines of evidence have begun to suggest that post-transcriptional mechanisms may also be important for regulation of IGF-IR expression (19,20). Cooke and Casella (21) provided the first specific evidence that translation of the IGF-IR mRNA could be regulated through its extraordinarily long (1038 nt) 5′-untranslated region (5′-UTR). More recently, IGF-IR was identified by microarray analysis as one of a group of candidate genes that might be regulated at the translational level (22).

Complex 5′-untranslated RNA sequences such as that associated with the IGF-IR mRNA (23,24) are rare in the human genome, generally reserved for the transcripts of genes critically involved in the control of cellular proliferation and survival (e.g. transcription factors, cytokines, growth factors and their receptors) (25,26). These complex 5′-UTR RNA sequences tend to adopt higher-ordered structures, which may dramatically influence translation efficiency. In addition to the structural features of the 5′-UTR RNA itself, non-canonical translation factors that interact with specific 5′-UTR RNA sequences are increasingly being recognized as important participants in translational regulation (27–33). These RNA-binding proteins can influence RNA secondary structure as well as the binding of other regulatory proteins to the RNA (34–36), and the position of the protein binding site within the 5′-UTR may determine the manner in which it influences translation efficiency (37–40).

We have begun to investigate the mechanisms of translational regulation through the complex IGF-IR 5′-UTR. We recently reported the detection and characterization of a diverse series of proteins interacting specifically with the human IGF-IR 5′-UTR (41). We proposed that the dynamic interplay between RNA structure and regulatory protein binding would be important in determining the functional state of the IGF-IR mRNA. Here, we report the purification and identification of one of these IGF-IR 5′-UTR RNA-binding proteins as HuR. HuR has been extensively characterized as a factor which enhances mRNA stability through binding to consensus AU-rich elements (ARE) in 3′-UTR sequences (42–45); however, a few recent reports have attributed HuR with the capability of either positively or negatively influencing translational efficiency (46,47). We present both *in vitro* and intracellular data to show that HuR functions as a translational repressor through interaction with its target sites within the IGF-IR 5′-UTR. We demonstrate that HuR inhibits both cap-dependent and internal ribosome entry site (IRES)-mediated translation initiation, but that these two mechanisms of translation repression are kinetically distinguishable. Our results indicate that HuR may play a very important role in the regulation of IGF-IR expression at the translational level.

MATERIALS AND METHODS

Plasmids

The firefly luciferase coding sequence was amplified by PCR from plasmid pGL3 (Promega) using primers Luc-A-Bgl II (5′-CTG **AGA TCT** ACC ATG GAA GAC GCC AAA-3′) and Luc-B (5′-GAA TTA CAC GGC GAT CTT TC-3′). The PCR product was inserted into the TA cloning site of plasmid pCR3.1 (Invitrogen) to generate plasmid pFLuc, in which the luciferase coding sequence is positioned downstream of the cytomegalovirus (CMV) and T7 promoters.

The full-length human IGF-IR 5′-UTR (+1 to 1038) was PCR amplified from normal human genomic DNA using primers IGFIR-B-KpnI (5′-TAA **GGT ACC** AGT GTG TGG CAG CGG CG-3′) and IGFIR-G-BglII (5′-GCG **AGA TCT** TCC TTT TAT TTG GGA TGA AAT TC-3′). The IGF-IR 5′-UTR fragment (+890 to 1038) was PCR amplified using primers IGFIR-KpnI-ApaI (5′-GAT GGT ACC CCG CCT TCG GAG TAT TGT TT-3′) and IGFIR-G-BglII. These PCR products were cloned into plasmid pFLuc using the KpnI and BglII restriction sites and the resulting plasmids were designated pIGFIR(1–1038)-FLuc and pIGFIR(890–1038)-FLuc, respectively. The plasmid pIGFIR(1–209)-FLuc was generated by re-ligation of plasmid pIGFIR(1–1038)-FLuc following digestion with BamHI and BglII.

The bi-cistronic reporter used to study the IRES activity of the IGF-IR 5′-UTR was constructed as follows: the *Renilla* luciferase coding sequence was PCR amplified from plasmid pRL-CMV (Promega) using primers Hind-RLuc-A (5′-GAC **AAG CTT** CAG GTA AGT ATC AAG GTT ACA-3′) and KpnI-RLuc-B (5′-GAC **GGT ACC** TTA TTG TTC ATT TTT GAG AAC TC-3′). The PCR product was cloned into plasmid pIGFIR(1–1038)-FLuc using the HindIII and KpnI sites. In this plasmid, the full-length human IGF-IR 5′-UTR sequence is positioned between the *Renilla* luciferase coding sequence (first cistron) and the firefly luciferase coding sequence (second cistron).

In vitro RNA synthesis

The plasmids pFLuc, pIGFIR(1–1038)-FLuc, pIGFIR(890–1038)-FLuc and pRL-CMV were linearized by XbaI to serve as templates to generate reporter RNAs for *in vitro* translation assays. Reporter RNAs were synthesized using the RiboMAX System (Promega). Briefly, in each 20 μl reaction, 2 μg DNA template was transcribed by T7 polymerase in the presence of 7.5 mM UTP, CTP, ATP and GTP. Capped RNA transcripts were synthesized in the presence of 2 mM cap analog (m^7GpppG) and 1 mM GTP. After 4 h incubation at 37°C, the reaction was stopped by adding 2 U of RNase-free DNase I for 30 min at 37°C. The RNA was purified by phenol/chloroform extraction and ethanol precipitation with 300 mM sodium acetate at −70°C overnight. RNA concentration was measured by conventional UV spectrometric analysis and agarose gel electrophoresis.

RNA crosslinking/RNase elution affinity purification

Synthesis of the biotin- and [α-^{32}P]UTP-labeled intact 1038 nt IGF-IR 5′-UTR RNA sequence was accomplished by *in vitro* transcription as described elsewhere (41), except that biotin-14-CTP was used in a 1:1 ratio with CTP (0.25 mM each)

Table 1. Comparison of the efficiency of RNA capture and recovery using different protocols or reagents for biotin labeling of RNA

	10% Bio-CTP	50% Bio-CTP	75% Bio-ATP
Starting material	100	100	100
Loading efficiency	58	92	63
After wash 2	54	87	55
After wash 3	50	85	50
Elution efficiency	42	67	40

The results of pilot experiments used to gauge the optimal method for biotin incorporation into target RNA. We anticipated that too low a level of biotin incorporation would result in limited capture of RNA molecules by the streptavidin–agarose matrix, while too high a level of biotin incorporation could potentially limit recovery of RNA-crosslinked protein. Satisfactory recovery of the RNA-binding protein upon RNase elution depends critically on RNase cleavage on both sides of the target RNA sequence and between adjacent points of biotin–streptavidin attachment to the matrix. The input of biotinylated ribonucleotide (bio-14-CTP or bio-17-ATP) relative to standard ribonucleotide (CTP or ATP) in the *in vitro* biosynthesis of the IGF-IR 5′-UTR is indicated. The data represent the relative percentage of radiolabeled RNA bound to matrix or recovered at various points in the RNA crosslinking/RNase elution protocol.

(see Table 1 for titration of the optimal degree of biotin incorporation), unlabeled UTP was increased to 100 μM, the incubation continued for a 4 h period and RNase inhibitor was omitted. Following synthesis, the double-labeled RNA was purified by dilution and filtration twice (Centricon, 100 kDa molecular weight cutoff). The double-labeled RNA was then incubated with HeLa nuclear extract and crosslinking was performed as previously described for qualitative assays (41), except that RNase digestion was omitted.

Briefly, HeLa nuclear extract was preincubated with 2% 2-mercaptoethanol at room temperature for 10 min. The pretreated extract was then added to reaction buffer [final concentration—40mM Tris, pH 7.4, 60 mM KCl, 5 mM $MgCl_2$, 1 mM spermidine, supplemented with 0.75 mM ATP, 0.75 mM GTP, 0.05% NP-40, non-specific competitors 0.1 μg/μl poly d(I–C) and 1 μg/μl tRNA] and incubated at room temperature for 10 min. The double-labeled RNA was then added to the reaction, and this incubation continued for 25 min at room temperature to allow for the formation of specific RNA–protein complexes. Subsequently, 5 mg/ml heparin was added to the reaction (10 min, room temperature) to eliminate weak or unstable RNA–protein interactions, after which the samples were irradiated (254 nm, 10 cm distance from source, Stratalinker, Model 1800) on ice for 25 min.

Then, the biotin- and radio-labeled 5′-UTR with protein crosslinked was incubated with streptavidin–agarose beads to immobilize the RNA. The streptavidin–agarose beads (Life Technologies) had been pre-equilibrated with RNA binding buffer (50 vol; 40 mM Tris pH 7.4, 1 mM EDTA, 80 mM KCl, 6% glycerol, 0.05% NP-40, 100 mM 2-mercaptoethanol) and blocked with blocking buffer (5 vol; binding buffer plus 0.25 mg/ml tRNA, 500 μg/ml BSA) before loading of the RNA–protein complexes. The efficiency of RNA–protein complex binding to streptavidin–agarose beads was determined by monitoring ^{32}P radioactivity in the flowthrough. We found that ∼90% of the RNA–protein complex was bound to the beads after 30 min gentle rocking in a 2 ml polypropylene microfuge tube at room temperature.

Because the protein was covalently crosslinked to the RNA, and the streptavidin–biotin linkage is highly stable, it was possible to use a washing protocol of extremely high stringency. The beads were pelleted by centrifugation for 3 min in a microfuge at low speed, and washed sequentially in 50 vol binding buffer (=washing buffer 1), 15 vol washing buffer 2 (binding buffer without KCl, plus 2% SDS), 15 vol prebinding buffer (binding buffer without KCl, to remove detergent), 15 vol washing buffer 3 (binding buffer with 1M KCl), and 15 vol binding buffer (to remove high salt). Finally, specific elution of bound RNA–protein complex was achieved under otherwise low-stringency conditions by the addition of 5 vol elution buffer [binding buffer plus 4 μg RNase A (Ambion, affinity purified)]. The eluted protein–oligoribonucleotide complex was concentrated to 50 μl by microfiltration through a 5% Tween-20 passivated Microcon YM-3 microfilter (Millipore). The purified protein, still attached to a small remnant of radiolabeled RNA, was resolved by 10% SDS–PAGE and detected by autoradiography.

Because the protein–oligoribonucleotide complex was radiolabeled, it was possible to readily follow the progress and evaluate the efficiency of recovery at each step, even on small and medium-scale purification trials, performed using reaction volumes between 8 and 800 μl and total protein of 20 ug to 2 mg. For large scale purification, the reaction was scaled up as much as 800-fold, RNA excess was ensured and its specific activity was reduced to minimize radiolysis, utilizing as much as ∼200 pmol total double-labeled RNA and ∼16 mg total HeLa nuclear extract in an 8 ml crosslinking reaction, loaded onto 200 μl streptavidin–agarose beads. Detection and excision of the RNA-binding proteins from the SDS–PAGE gel were performed by aligning the autoradiographic film with the gel (without any staining). Using this strategy, starting with a relatively small amount of crude nuclear extract, we were able to enrich for even a minor component in the crosslinking/label transfer reaction to a degree sufficient for positive identification by tandem mass spectrometry.

Protein isolation and tandem mass spectrometry analysis

The band representing the 38 kDa RNA binding protein eluted from the RNA affinity matrix, and a control, which was excised from an adjacent control lane, were subjected to *de novo* peptide sequence analysis by Dr William S. Lane, Harvard Microchemistry Facility. Briefly, the trypsin-digested peptides were separated by microcapillary reverse-phase high-performance liquid chromatography, which is directly coupled to the nano-electrospray ionization source of an ion trap mass spectrometer. The MS/MS spectra were then correlated with known sequences using the Sequest algorithm.

Recombinant HuR

Bacterially expressed HuR. The cDNA for HuR was subcloned into pGEX-5X-1 (Amersham) in frame with the GST tag. The plasmid was transformed into the BL21 strain of *Escherichia coli* and the protein was purified as described previously (48). Recombinant GST (also the *Schistosoma*

japonicum sequence), which served as a control, was purchased from Sigma.

In vitro translated HuR. The plasmid pcDNA3-HuR (a generous gift of J. A. Steitz) was linearized by PspOM I to serve as the template for *in vitro* transcription of RNA encoding full-length untagged human HuR. Recombinant HuR to be used in *in vitro* translation assays was prepared using 1 μg HuR RNA in a standard RRL reaction. This *in vitro* translation reaction was stopped by adding 2 U of micrococcal nuclease (Amersham) and 1 μl $CaCl_2$ (20 mM), and incubated at room temperature for 15 min. Micrococcal nuclease was inactivated by adding 1 μl EGTA (40 mM). The *in vitro* synthesized HuR protein was frozen in dry ice/ethanol and stored at −70°C.

Immunoprecipitation

UV crosslinking was performed as described previously (41). The RNase digested UV crosslinked samples (20 μl, containing ~50 μg HeLa nuclear extract) were then incubated with RIPA buffer (1 ml; 1× PBS, 1% NP-40, 0.1% SDS), control IgG (1 μg) and protein A/G plus-agarose beads (20 μl, Santa Cruz) at 4°C for 30 min. The precleared supernatant was then incubated with 1 μg HuR antibody (3A2, Santa Cruz) or isotype-matched irrelevant control antibody (Sp1, Santa Cruz) at 4°C for 60 min. Subsequently, 20 μl of protein A/G plus-agarose beads were added and further incubated at 4°C for 4 h. After washing four times with 1 ml RIPA buffer, the beads were pelleted by centrifugation and boiled in protein sample buffer, and the samples resolved on 10% SDS–PAGE.

Western-shift assay

The IGF-IR 5′-UTR RNA was incubated with nuclear extract, and samples subjected to a standard UV crosslinking/label transfer protocol, including RNase digestion. Samples were then separated on 10% SDS–PAGE and transferred to 0.2 μm nitrocellulose membrane. Blots were probed with monoclonal antibody to HuR (3A2, Santa Cruz) at a 1:125 dilution in blocking buffer (5% non-fat dry milk in TBS–Tween buffer). Horseradish peroxidase-conjugated secondary antibody (anti-mouse IgG) was used at a 1:5000 dilution in blocking buffer. The signal was detected by enhanced chemiluminescence (ECL, Amersham). Although the RNA used for the Western-shift assay was radiolabeled, as it is for crosslinking, the only bands visible on the western-shift image are those produced by chemiluminescence, exposing the blot to film for a period of only seconds to a few minutes. Autoradiographic development would have required overnight exposure at −70°C with intensifying screen.

In vitro translation assay

In vitro translation assays were performed using Flexi Rabbit Reticulocyte Lysate (Promega). Each 20 μl reaction contained 14 μl rabbit reticulocyte lysate (RRL), 0.2 μl amino acid mixture minus leucine, 0.2 μl amino acid mixture minus methionine, and 0.56 μl 2.5M KCl. Recombinant HuR was pre-incubated with the reporter RNA for 10 min at room temperature before initiation of the translation reaction. The samples were incubated at 30°C for 90 min (standard) or otherwise as indicated in the figure legends, and the reactions were stopped by adding RNase A.

Translation velocity V_{transl} was calculated according to the following formula:

$$V_{\text{transl}} = \frac{(L_{n+1} - L_n)}{(t_{n+1} - t_n)},$$

where L is luciferase activity for a given sample, t is time and n and $n + 1$ represent any two consecutive time points. Data are plotted against the midpoint between the two adjacent time points used to calculate V_{transl}.

Cell culture and transient transfection

OVCAR3 cells (human ovarian carcinoma) were grown in DMEM supplemented with 10% fetal calf serum, vitamins, glutamine and penicillin/streptomycin. Cells were propagated using standard culture techniques and maintained in a humidified 37°C, 5% CO_2 environment. Transfection was performed using calcium phosphate precipitation. All transfections were performed in triplicate on at least three independent experiments.

Luciferase assays

The firefly and *Renilla* luciferase activities within lysates of transfected cells or produced by the *in vitro* translation assay were measured using the Dual-Luciferase Reporter Assay System (Promega). All measurements were performed using the TD-20/20 luminometer (Turner Designs).

RNase protection assays

The ^{32}P-CTP internally labeled antisense RNA probes for firefly and *Renilla* luciferase coding sequences were synthesized by *in vitro* transcription. The firefly luciferase template was generated by linearizing the pSP-luc+NF plasmid (Promega) by HincII. The *Renilla* luciferase template was generated by PCR, with T7 promoter incorporated into the reverse primer. The primer sequences are (forward) ATCCAACTCGCAGAATCCAACTCGCAGCCTTGAGCCAGTAGCGCGGTGTA, (reverse) ACTGTAATACGACTCACTATAGGGAGACACTTTCAGCGTGAACTATTGCT.

Total RNA from transfected cells was recovered using TRIzol reagent (Invitrogen), assessed qualitatively by agarose gel electrophoresis and quantitated spectrophotometrically. Equal aliquots (6 μg total RNA) were included in solution hybridization reactions (RPA III, Ambion) with antisense probes for the firefly or *Renilla* luciferase coding sequences at 42°C overnight. Following digestion with RNases A plus T_1 (1:100 dilution) at 37°C for 30 min, protected RNA was recovered by precipitation and resolved on a 5% polyacrylamide, 8 M urea sequencing gel, and the results were obtained by autoradiography. Relative band intensities were quantified using the ScionImage (NIH Image) program.

siRNA knockdown of HuR

A combination of four chemically synthesized siRNA duplex molecules targeted to the human HuR mRNA sequence (Dharmacon) was transiently transfected (final concentration 50 nM) into OVCAR3 cells (70% confluent in six-well plates) using Oligofectamine and OptiMEM serum-free medium (Invitrogen). siRNA targeted to EGFP was used as a control. Forty-eight hours after transfection, whole-cell lysates were

prepared for assessment of HuR, IGF-IR and alpha-tubulin levels by immunoblot (using primary antibodies 3A2, C-20 and B-5-1-2, respectively).

Pilot experiments utilized HuR-targeted siRNA modified with the fluorescent dye Alexa Fluor 647 (Ulysis reagent, Molecular Probes) to gauge transfection efficiency, which was ~100%.

HuR truncation mutants

A series of five *in vitro* expression cassettes encoding the full-length (untagged) HuR protein or four C-terminal truncations were prepared by PCR amplification from the parent plasmid pcDNA3-HuR. The common plus-strand primer hybridized upstream of the T7 promoter, whereas each of the downstream primers (except that for the full-length protein) introduced a premature in-frame stop codon into the HuR coding sequence. The wild-type and mutant recombinant proteins were generated by sequential *in vitro* transcription and translation reactions.

RESULTS

Design and implementation of a novel RNA crosslinking/RNase elution strategy for purification and identification of the regulatory proteins binding the IGF-IR 5′-UTR

Recently, we reported the results of an extensive series of *in vitro* crosslinking/label transfer experiments in which we detected and characterized a series of putative regulatory proteins present in various human cellular extracts which are capable of binding specifically to the IGF-IR 5′-UTR sequence under highly stringent conditions (49). In our quest to identify the IGF-IR 5′-UTR binding proteins, we adapted some of the features of the crosslinking/label transfer procedure to develop a new protocol for affinity purification of these proteins from crude cellular extract (Figure 1A and Table 1). The essential features of this strategy involve covalent crosslinking of the RNA-binding protein to its target RNA sequence (in the presence of nonspecific competitor nucleic acids and heparin), an extremely high-stringency washing protocol (including

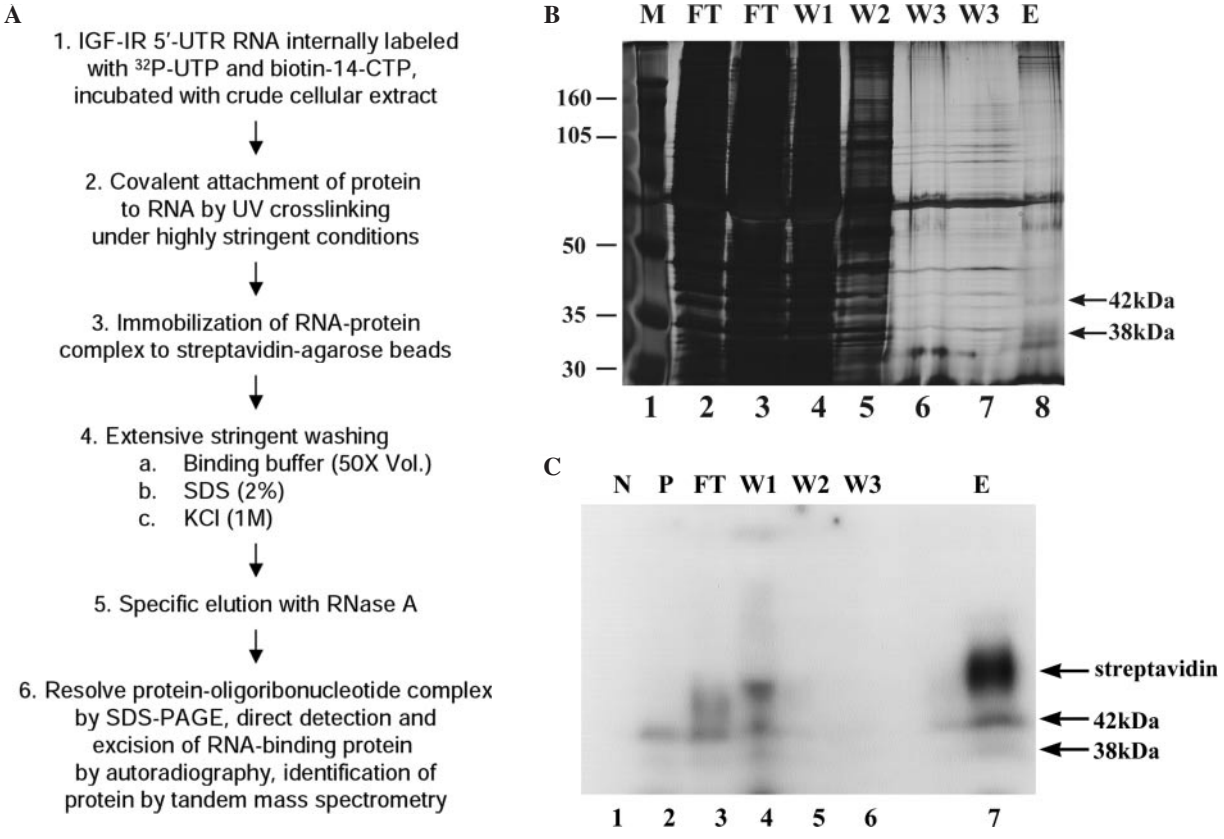

Figure 1. RNA crosslinking/RNase elution strategy for purification and identification of the regulatory proteins binding the IGF-IR 5′-UTR. (**A**) Diagram of the essential features of the protocol developed and used to enrich and identify RNA-binding proteins potentially regulating IGF-IR expression at the translational level (see Materials and Methods for details). (**B**) The silver-stained SDS–PAGE gel from a medium-scale preparative trial reveals the high degree of enrichment for the specific RNA-binding proteins relative to total cellular protein attained using this protocol. FT, flowthrough; W1, wash #1 (50 vol binding buffer); W2, wash #2 (containing 2% SDS); W3, wash #3 (containing 1 M KCl); E, elution (RNase A in binding buffer). The positions of the 38 and 42 kDa proteins (in the eluate) which bind specifically to the IGF-IR 5′-UTR [as previously described (41)] are indicated to the right. The positions of the molecular weight markers are indicated to the left. The band seen just below the 38 kDa band was determined to be a contaminant of the RNase (observed with RNase alone). (**C**) Autoradiograph of an unstained gel (as was used to guide excision of the bands for tandem mass spectrometric analysis) demonstrating the IGF-IR 5′-UTR-binding proteins. N, negative control (no UV crosslinking); P, positive control (input), a small aliquot of the sample, removed before loading on the matrix. The positions of the 38 and 42 kDa proteins are indicated by the arrows on the right. [Note that the HuR–oligoribonucleotide complex (38 kDa) was actually a relatively low-intensity band in the crosslinking/label transfer reaction. Identification of the more predominant 42 kDa crosslinked band will be reported in a separate communication.] The position of the inadvertently released streptavidin tetramer (~60 kDa, complexed with remnant oligoribonucleotides) is indicated as well.

2% SDS followed by 1 M KCl) and specific elution under otherwise low-stringency conditions through enzymatic digestion of the matrix-bound RNA.

A very high degree of enrichment for the RNA-binding proteins from crude nuclear extract is evident in a silver-stained gel of the various fractions resulting from a medium-scale purification trial (Figure 1B). Although some loss in the flowthrough and initial low-stringency wash was noted, it was possible to recover a considerable proportion of the specifically crosslinked 38 and 42 kDa proteins in the final elution step (autoradiograph, Figure 1C). Because detection of the protein depended on covalent attachment to a radiolabeled remnant of its RNA target sequence, this ensured that the band excised from the SDS–PAGE gel was in fact the RNA-binding protein of interest, and made it possible to avoid the decrement in quality of mass spectrometric data associated with silver staining (50,51).

Tentative identification of the 38 kDa IGF-IR 5′-UTR-binding protein as HuR

The results of tandem mass spectrometry performed on the 38 kDa band isolated using the RNA crosslinking/RNase elution protocol yielded four different peptide sequences (21% sequence coverage, Table 2) which matched the human protein HuR (44). HuR (also known as HuA) is one of four members of the human Hu protein family, which are highly homologous to the *Drosophila* ELAV (embryonic lethal abnormal vision) proteins (52). Whereas the other three family members, HuB, HuC and HuD, are specifically expressed in neural tissues, HuR is expressed ubiquitously (44). HuR contains three RNA recognition motifs (RRMs) (53) and a hinge region between RRM2 and RRM3 which has been characterized as the HuR nuclear–cytoplasmic shuttling sequence (54).

Confirmation that the 38 kDa protein binding to the IGF-IR 5′-UTR is HuR

Three independent methods were employed to confirm that the 38 kDa protein, which we have previously characterized as binding to the IGF-IR 5′-UTR, is in fact HuR. First, we showed that the 38 kDa band produced by UV crosslinking of cellular protein to the IGF-IR 5′-UTR could be specifically immunoprecipitated by a monoclonal antibody to HuR, but not by an isotype-matched irrelevant control antibody (Figure 2A and data not shown). We found that the efficiency of immunoprecipitation of the 38 kDa crosslinked RNA–protein complex actually increased slightly in the presence of the detergent Empigen BB, which selectively disrupts physiological protein–protein interactions without disturbing high-affinity antibody–antigen interactions (55). Thus this result confirms the direct interaction of HuR with the IGF-IR 5′-UTR RNA.

Table 2. HuR peptide sequences identified by tandem mass spectrometric analysis of the 38 kDa band enriched through use of the RNA crosslinking/RNase elution protocol

	Peptide sequence	Position in HuR	Domain
1	TNLIVNYLPQNMTQDELR	20–37	RRM1
2	SLFSSIGEVESAK	38–50	RRM1
3	VLVDQTTGLSR	137–147	RRM2
4	SEAEEAITSFNGHKPPGSSEPITVK	158–182	RRM2

The amino acid position and structural domain localization of each peptide is indicated. These four peptides represent 21% coverage for the human HuR sequence (accession number: XP_008947). RRM = RNA recognition motif.

Next we examined the capacity of purified recombinant GST-HuR to bind specifically to the IGF-IR 5′-UTR RNA (Figure 2B). GST-HuR (62 kDa) interacts directly with the IGF-IR 5′-UTR sequence while recombinant GST alone does not. This result, performed in the absence of other eukaryotic proteins, also indicates that HuR is capable of binding to the IGF-IR 5′-UTR independently of any putative auxiliary factors.

We also used a series of 5′ and 3′ deletions of the IGF-IR 5′-UTR RNA to map the binding sites for recombinant GST-HuR (Figure 2C). Recombinant HuR exhibited precisely the same mapping characteristics as the cellular 38 kDa RNA-binding protein (41), with its binding sites localized to the 3′-most 149 nt of the 5′-UTR (890–1038). Within this region, two short U-rich sequences and one long polypyrimidine tract have been identified as candidate HuR binding sites.

We also developed a new method, which we have designated the western-shift assay, to demonstrate the binding of cellular HuR to the IGF-IR 5′-UTR. Crosslinking of a specific cellular RNA-binding protein to its target sequence, followed by RNase T_1 digestion (which cleaves after unpaired G residues), will leave a residual oligoribonucleotide covalently attached to the RNA-binding protein. This will result in an effective shift of the molecular weight of the RNA-binding protein attributable to the remnant of the target RNA, which should be detectable by western blot analysis. Indeed, native HuR bands shifted by covalent attachment to remnants of the IGF-IR 5′-UTR were observed [Figure 2D, compare lane 3 (with no crosslinking) to lane 4], and the intensities of the shifted bands progressively increased with increasing input of the IGF-IR 5′-UTR RNA (lanes 5–8). If the crosslinked RNA–protein complex was further digested by RNase A (which cleaves after pyrimidines), the size of the residual crosslinked oligoribonucleotide and thus the relative shift of molecular weight was dramatically reduced (lanes 1 and 2).

There were at least three advantages of the western-shift assay for confirmation of the identity of a specific RNA-binding protein which are worthy of mention. First, this technique does not require the use of recombinant proteins, which in many cases have been observed to lose their RNA-binding activity or specificity *in vitro* (56). Second, no immunoprecipitation-competent antibody was required. Finally, the western-shift assay allows direct quantitative assessment of the binding capacity of a cellular protein to a specific RNA molecule, which is not possible with standard crosslinking/label transfer experiments, in which neither the unbound RNA nor the unbound protein is visualized.

Together these results provide confirmation that the 38 kDa IGF-IR 5′-UTR-binding protein is HuR.

HuR inhibits translation through the IGF-IR 5′-UTR *in vitro*

We had hypothesized that the proteins binding the complex 5′-UTR of the IGF-IR transcript would contribute to the regulation of IGF-IR expression at the translational level. To examine the effect of HuR on IGF-IR translation, we first performed

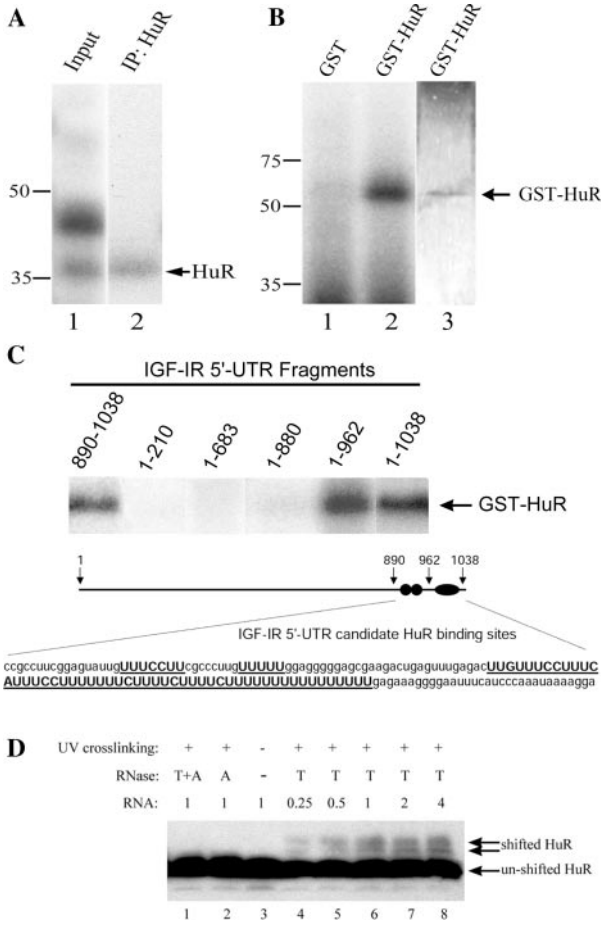

Figure 2. Confirmation that the 38 kDa IGF-IR 5′-UTR-binding protein is HuR. (**A**) Specific immunoprecipitation of the 38 kDa UV-crosslinked band by a monoclonal antibody to HuR. Lane 1 is a representative result of the crosslinking/label transfer procedure demonstrating two of the proteins binding specifically to the intact IGF-IR 5′-UTR RNA. In lane 2, the products of the UV crosslinking reaction were subjected to immunoprecipitation using a monoclonal antibody to HuR (3A2) in the presence of Empigen (1%). An isotype-matched irrelevant antibody used as a control yielded a negative result (data not shown). Note that the more predominant 42 kDa band was not co-immunoprecipitated with HuR. (**B**) Specific binding of recombinant HuR to the IGF-IR 5′-UTR. UV crosslinking was performed following incubation of either purified GST-HuR or GST with the labeled IGF-IR 5′-UTR. GST-HuR (Lane 2), but not GST alone (Lane 1), bound to the IGF-IR 5′-UTR, producing a single ∼62 kDa band. Lane 3 is the result of silver staining of Lane 2, demonstrating the purity and relative amount of the recombinant GST-HuR preparation. (**C**) Localization of the HuR binding sites within the IGF-IR 5′-UTR. A series of fragments of the IGF-IR 5′-UTR was tested in the UV crosslinking assay to map the binding sites for recombinant GST-HuR. The UV crosslinking data are shown above. The position of three candidate HuR binding sites (symbolized by ellipses), including two short U-rich sequences and one very long polypyrimidine tract within the 890–1038 nt IGF-IR 5′-UTR sequence, are shown below. (**D**) Demonstration of binding of cellular HuR to the IGF-IR 5′-UTR by altered mobility on immunoblot (western-shift assay). The IGF-IR 5′-UTR was incubated with nuclear extract, and crosslinking followed by RNase T_1 digestion performed under highly stringent conditions as described in Materials and Methods. The products of the crosslinking reaction were separated on SDS–PAGE. Following transfer to a 0.2 μm nitrocellulose membrane, the blot was probed with antibody to HuR (3A2). Lane 3: native HuR protein (not crosslinked to RNA). Lanes 4–8: HuR protein UV crosslinked to increasing amounts of IGF-IR 5′-UTR RNA and digested by RNase T1. Lanes 1 and 2: HuR UV crosslinked to IGF-IR 5′-UTR and digested by RNase T1 and A together or RNase A alone. The relative concentration of the RNA is indicated above each lane, and the positions of native HuR as well as HuR shifted by crosslinking to a remnant of the IGF-IR 5′-UTR RNA target sequence are indicated by arrows.

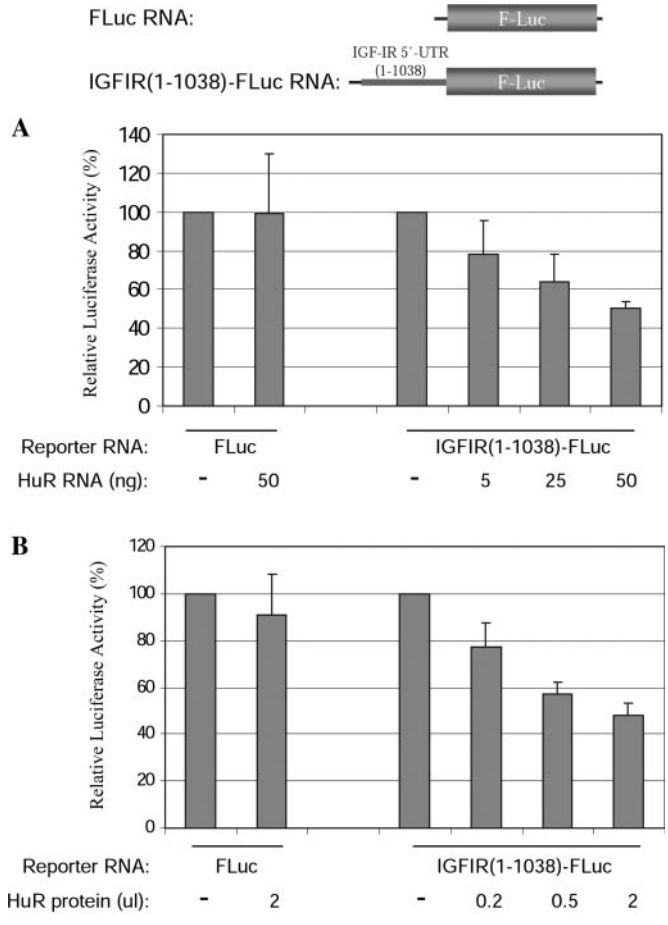

Figure 3. HuR specifically represses translation through the IGF-IR 5′-UTR in a concentration-dependent manner. (**A**) *In vitro* co-translation assay. The IGFIR(1–1038)-FLuc RNA (5 ng) was incubated with increasing amounts of *in vitro* transcribed mRNA encoding HuR (5–50 ng) in an *in vitro* translation reaction (with RRL). The FLuc RNA (5 ng) was used as a control. The results are expressed relative to the control reactions without HuR. (**B**) *In vitro* translation with recombinant HuR protein. HuR protein (no tag) was synthesized *in vitro* as described in Materials and Methods. Increasing amounts of HuR protein were included in the *in vitro* translation assay using the IGFIR(1–1038)-FLuc reporter RNA. HuR protein progressively decreased translation of the reporter RNA containing the full-length IGF-IR 5′-UTR but, even at the highest concentration used, had no significant effect on translation of the control luciferase reporter RNA.

an *in vitro* co-translation assay, in which the RNA encoding HuR and the reporter RNA containing the full length IGF-IR 5′-UTR (positioned upstream of the firefly luciferase coding sequence) were incubated together in RRL. Inclusion of the HuR RNA specifically decreased translation of the reporter RNA containing the IGF-IR 5′-UTR in a concentration-dependent manner, whereas the HuR RNA had no effect on the translation of a control reporter RNA with no IGF-IR 5′-UTR sequence (Figure 3A). To demonstrate the inhibitory effect of HuR on IGF-IR translation more directly, we next added *in vitro* translated HuR protein directly to the *in vitro* translation assay. As shown in Figure 3B, the recombinant untagged HuR protein specifically inhibited translation of the IGF-IR 5′-UTR reporter RNA in a similar manner as observed in the co-translation assay. These results indicate that HuR is capable of negatively influencing translation efficiency *in vitro* through the IGF-IR 5′-UTR.

To further establish the sequence-specificity of translational repression by HuR, we used an isolated 149 nt fragment of the IGF-IR 5′-UTR (nt 890–1038), which encompasses the HuR binding sites, as a specific competitor for HuR in the *in vitro* translation assay. With increasing amount of the competitor RNA added, the inhibitory effect of HuR on translation through the IGF-IR 5′-UTR was progressively diminished (Figure 4A). However, a similarly sized fragment of the IGF-IR 5′-UTR (nt 1–205), which does not bind HuR, had no such effect.

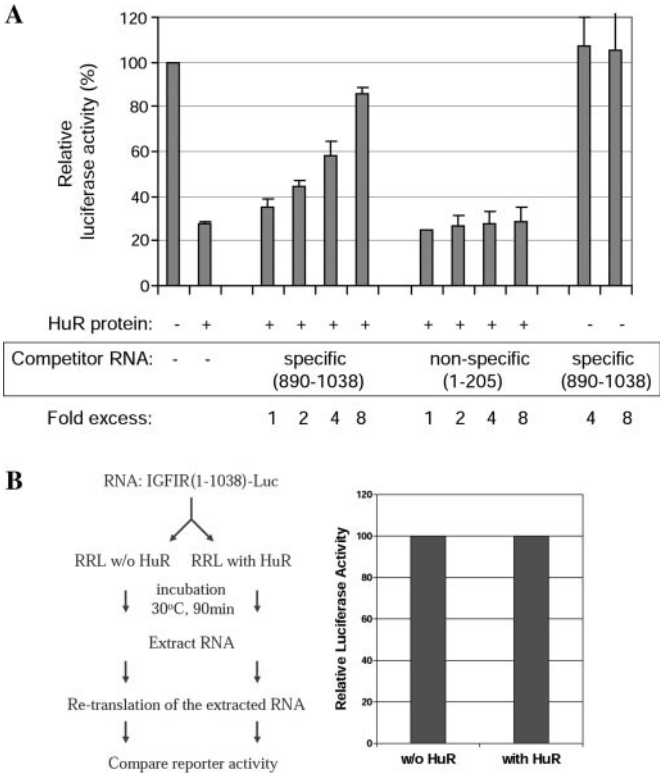

Figure 4. Translational repression by HuR is accomplished through direct interaction with its binding sites within the IGF-IR 5′-UTR and does not involve permanent alteration of the RNA. (**A**) *In vitro* translation assays were performed using the IGF-IR 5′-UTR reporter and recombinant HuR as described above, except that in these experiments, an isolated 149 nt RNA fragment (nt 890–1038) of the IGF-IR 5′-UTR, which includes all the high-affinity HuR binding sites (refer to Figure 2C), was included as a specific competitor for HuR binding and translational repression. The specific competitor RNA relieved the inhibitory effect of HuR on translation through the IGF-IR 5′-UTR in a concentration-dependent manner. In contrast, another similarly sized fragment of the native IGF-IR 5′-UTR (nt 1–205), which is devoid of HuR binding sites, had no effect on HuR translational repression. The last two bars represent addition of specific competitor RNA in the absence of HuR protein. The results rule out a general stimulatory effect of the specific competitor RNA on translation. *Renilla* RNA was included in all reactions as an internal control, and all firefly luciferase levels were normalized to *Renilla* luciferase levels. The results are expressed relative to the control reaction without HuR or competitor RNA. (**B**) Re-translation assay designed to test the effect of HuR on mRNA stability *in vitro*. IGFIR(1–1038)-FLuc RNA containing the full length IGF-IR 5′-UTR was incubated with or without HuR in an *in vitro* translation reaction. Following the first round of translation, RNAs were recovered by phenol/chloroform extraction and ethanol precipitation and were separately used as templates for a second round of *in vitro* translation in RRL. The results of the re-translation assay demonstrate that the prior incubation of the RNA with HuR has no residual effect on translation efficiency. This experiment was repeated using GST-HuR with essentially identical results.

The negative effect of HuR on translation through the IGF-IR 5′-UTR could conceivably be caused by decreased stability of these reporter RNAs (although in the literature, HuR has consistently been associated with stabilization rather than destabilization of RNA). To rule out this possibility, an *in vitro* re-translation assay was performed (57). As depicted in Figure 4B, the IGF-IR 5′-UTR reporter RNA was subjected to a first round of translation in the presence or absence of HuR protein, and then was extracted and re-translated. If HuR had decreased the reporter RNA stability, we would expect to detect a difference in the second round of translation. The result clearly indicated that these two populations of RNA still have exactly the same ability to be translated. Taken together, these results demonstrate that HuR specifically inhibits its translation *in vitro* through specific interaction with its target sequences within the IGF-IR 5′-UTR, without permanently altering the translatability of the RNA.

RRM3 is necessary for HuR translational repression

Next, we sought to delineate the structural domains of HuR responsible for translational repression. Four C-terminal truncation mutants of HuR were generated by *in vitro* translation, and the effects of each of these proteins on translation initiation through the IGF-IR 5′-UTR were measured (Figure 5). Interestingly, deletion of just the C-terminal 82 amino acids (RRM3) of HuR caused a dramatic reduction in translational repression, relative to the wild-type protein generated in the same manner (panel A). Further deletion of the nuclear–cytoplasmic shuttling sequence, or all or part of RRM2, had no further influence on HuR translation-regulatory function. Under conditions in which cap-dependent scanning is inhibited and only IRES-mediated translation initiation is measured (discussed extensively below), deletion of RRM3 completely abrogated HuR translational repression (panel B). Crosslinking analysis reveals a total loss of binding of HuR to the IGF-IR 5′-UTR upon deletion of RRM3 (panels C and D).

Taken together, these results indicate that RRM3 is critical for high-affinity sequence-specific binding to the IGF-IR 5′-UTR, and absolutely necessary for repression of IRES-mediated translation. The minimal residual translational repression observed with HuR RRM1 alone may be due to a low-affinity interaction with the IGF-IR 5′-UTR RNA (undetectable under the high-stringency conditions used for crosslinking).

HuR specifically inhibits translation through the IGF-IR 5′-UTR in cells

To determine whether HuR can function as a translation repressor in the intact cell, the IGF-IR reporter construct pIGFIR(890–1038)-FLuc and the expression plasmid for untagged HuR (43) were transiently co-transfected into the OVCAR3 cell line. HuR specifically inhibited translation of the reporter containing the HuR binding sequence (Figure 6A) but had no effect on translation of the reporter pIGFIR(1–209)-FLuc, which contains a similarly sized fragment of the IGF-IR 5′-UTR that does not bind HuR. Also, no such inhibitory effect was observed if an expression plasmid encoding a control RNA-binding protein, hnRNP C, was co-transfected with the IGF-IR 5′-UTR reporter. Importantly, the inhibitory effect of HuR on reporter expression was not accompanied by a

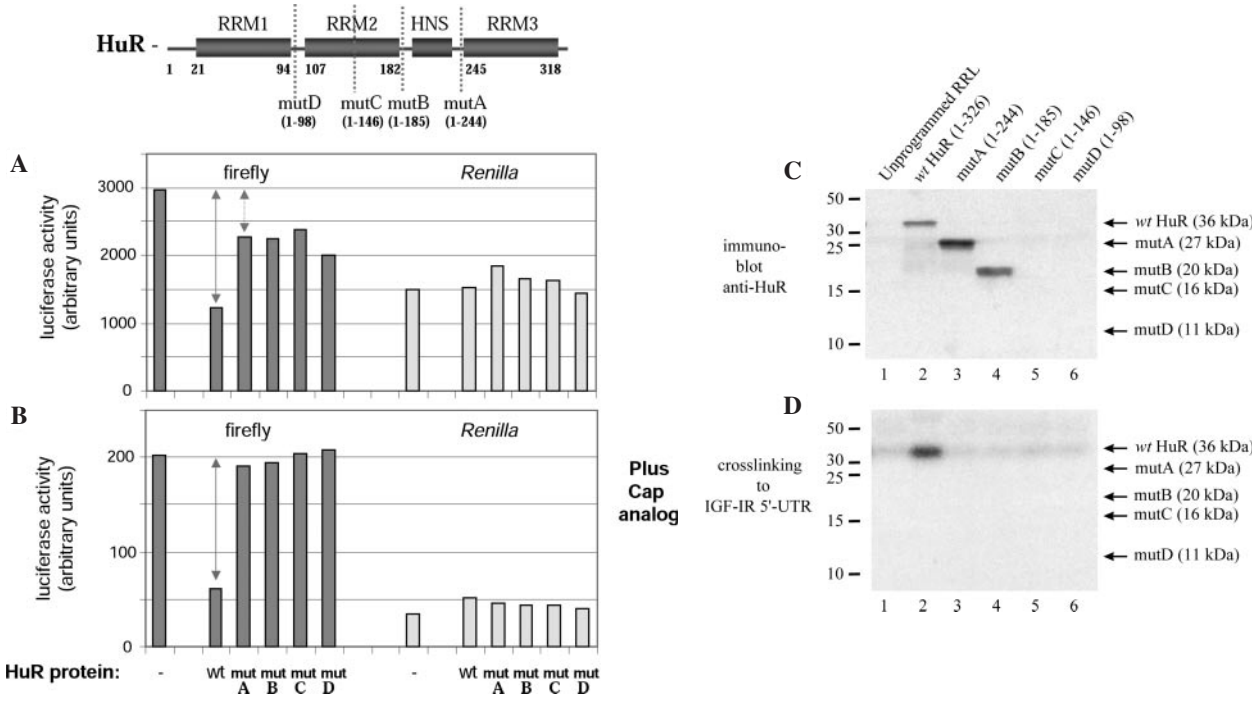

Figure 5. RRM3 is required for HuR translational repression. Full-length HuR and four C-terminal deletion mutants were prepared as described in Materials and Methods. The diagram above indicates the relative positions of the C-termini for each of the HuR truncation mutants. In mutA, RRM3 is selectively deleted. In mutB, the nuclear–cytoplasmic shuttling sequence is also removed. In mutC, RRM2 is bisected, whereas mutD retains only RRM1. (**A**) The capacity of each of these HuR truncation mutants to function as a translational repressor was measured by the standard *in vitro* translation assay [using the capped IGF-IR(890–1038)-FLuc reporter RNA] and compared with the full-length HuR generated in the same manner. *Renilla* luciferase reporter RNA was included in all reactions as an internal control, and the raw data are included (lightly shaded bars on the right). The solid arrow represents the degree of translational repression associated with wild-type HuR, and the dotted arrow represents the minimal residual translational repression observed with each of the C-terminal HuR truncation mutants, apparently attributable to RRM1 alone. (**B**) Cap analog (3 mM) was included an aliquot of 3 mM cap analog was included in the translation reaction, to inhibit cap-dependent translation initiation of the IGF-IR(890–1038)-FLuc reporter RNA. Thus, this assay specifically measures HuR repression of IRES-mediated translation (discussed in detail later in text). The double-headed arrow represents the degree of repression of IRES-mediated translation initiation observed with wild-type HuR. Note that the ability of HuR to repress IRES-mediated translation initiation is completely abrogated by deletion of RRM3. The experiment was repeated with nearly identical results. (**C**) Immunoblot analysis of the full-length HuR and C-terminal truncation mutants. Synthesis and accumulation of comparable quantities of the mutC and mutD proteins, which are not detectable with the 3A2 antibody, was confirmed by analysis of ^{35}S-labeled reaction products (data not shown). (**D**) Standard crosslinking analysis to measure binding of full-length and C-terminal truncation mutants of HuR to the IGF-IR 5′-UTR. Only the wild-type HuR yields a detectable crosslinked band (lane 2); the loss of RNA-binding activity accompanying deletion of RRM3 correlates well with the loss of translational repression (A and B).

concomitant decrease of the mRNA level (Figure 6B), confirming that the specific repression of gene expression by HuR through the IGF-IR 5′-UTR in cells occurs at the translational level.

HuR inhibits IGF-IR IRES-mediated translation

Recently, it has been reported that the rat IGF-IR 5′-UTR, which is 85% homologous to the human sequence, contains an IRES (58). We have now determined that the human IGF-IR 5′-UTR also contains a functional IRES (Z. Meng, C. Badorff, P. D. Emanuel and S. W. Blume, manuscript in preparation). The bi-cistronic dual-luciferase reporter used to measure IRES activity was also used to test whether HuR could inhibit translation mediated through the human IGF-IR IRES. In the dual-luciferase reporter, the *Renilla* luciferase (first cistron) will be translated in a cap-dependent manner, whereas the firefly luciferase (second cistron), which is preceded by the human IGF-IR 5′-UTR sequence, will be translated through internal ribosome entry. As shown in Figure 7, HuR significantly inhibited translation mediated by the IGF-IR IRES in a concentration-dependent manner in cells, whereas the control protein hnRNP C had no such effect.

HuR knockdown increases IGF-IR levels *in vivo*

The results described above, utilizing *in vitro* and intracellular reporter assays, demonstrate that recombinant HuR functions as a potent repressor of translation initiation mediated through the IGF-IR 5′-UTR. To confirm a similar functional relationship between endogenous HuR and endogenous IGF-IR in cells, siRNA knockdown experiments targeted to HuR were performed. Transfection of HuR siRNA into OVCAR3 cells resulted in a dramatic decrease in HuR levels, accompanied by a significant increase in IGF-IR levels (Figure 8). The control siRNA targeted to EGFP had no significant effect on either HuR or IGF-IR levels. These results provide substantial evidence that HuR indeed serves as a physiological regulator of IGF-IR expression *in vivo*.

Establishment of a quantitative *in vitro* system to investigate the mechanism of translational repression by HuR

Since IGF-IR translation through its complex 5′-UTR can be initiated by either the cap-dependent or IRES-mediated pathway, we speculated that HuR might utilize different mechanisms to repress each pathway. To this end, we elected

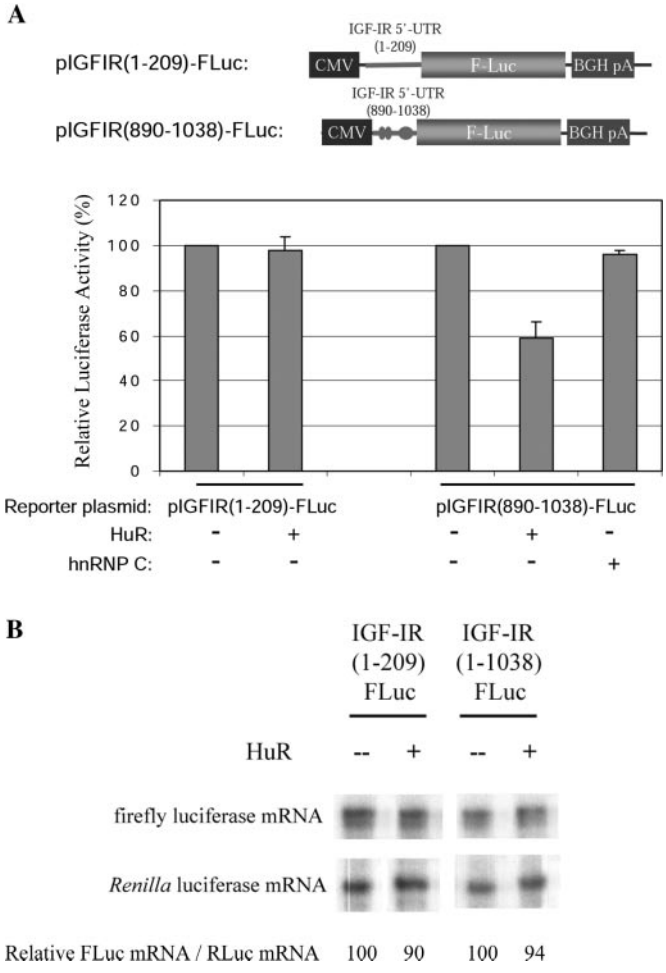

Figure 6. HuR specifically represses translation through the IGF-IR 5′-UTR in cells. (**A**) The expression plasmid for HuR (200 ng) was co-transfected with pIGFIR(890–1038)-FLuc (containing the HuR binding sites, represented by ellipses in the diagram above) or the control reporter construct [pIGFIR (1–209)-FLuc, no HuR binding sites] (100 ng) into OVCAR3 cells as indicated. Overexpression of HuR was confirmed by western blot analysis (data not shown). Cells were harvested 48 h after transfection and extracts analyzed for firefly luciferase expression. All firefly luciferase activities were normalized for transfection efficiency using a *Renilla* luciferase control vector. Assays were performed in triplicate and the experiment repeated three times. The results are presented relative to control samples with no ectopically expressed HuR. HuR specifically inhibited translation of the reporter containing its target sequences within the IGF-IR 5′-UTR. The control protein hnRNP C had no such effect. BGHpA: bovine growth hormone polyadenylation site. (**B**) Confirmation that HuR does not alter the level of reporter mRNA containing the IGF-IR 5′-UTR. Cells were co-transfected with either pIGFIR(1–1038)-FLuc or pIGFIR(1–209)-FLuc (no HuR binding sites), along with the expression plasmid for HuR or pcDNA3.1 (with no insert). The *Renilla* luciferase control vector was used as an internal control in all samples. Total RNA was harvested 48 h after transfection, and levels of the firefly and *Renilla* luciferase mRNAs in each cell sample were assessed by RNase protection (as described in Materials and Methods). Firefly luciferase mRNA levels were normalized for *Renilla* luciferase mRNA levels and quantified relative to that of cells in which HuR was not ectopically expressed.

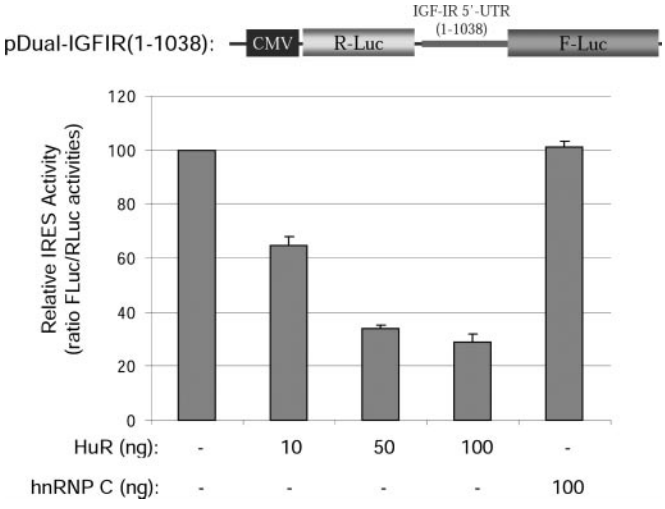

Figure 7. HuR inhibits IRES-mediated translation through the IGF-IR 5′-UTR. A bi-cistronic reporter construct was prepared in which the full-length human IGF-IR 5′-UTR sequence was positioned between the coding sequences for *Renilla* luciferase (first cistron) and firefly luciferase (second cistron). The bi-cistronic reporter plasmid (100 ng) was co-transfected with different amounts of the HuR expression plasmid (or hnRNP C expression plasmid as control) into OVCAR3 cells as indicated. The total amount of DNA transfected was kept constant by adding pcDNA3 plasmid. At 48 h post-transfection, the firefly and *Renilla* luciferase activities were measured. The FLuc:RLuc ratio of samples in which HuR or hnRNP C was ectopically expressed is presented relative to control samples with no ectopically expressed HuR. The assays were performed in triplicate and the experiment repeated three times.

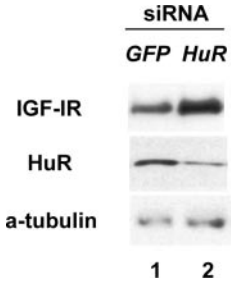

Figure 8. siRNA knockdown of endogenous HuR increases IGF-IR levels *in vivo*. OVCAR3 cells were transfected with a pool of four siRNA duplexes (final concentration 50 nM) targeted to the human HuR mRNA using Oligofectamine and serum-free medium as described in Materials and Methods. An equivalent concentration of siRNA targeted to EGFP served as a control. Forty-eight hours after transfection, whole-cell lysates were prepared and HuR, IGF-IR and alpha-tubulin levels were assessed by western blot. The experiment was repeated and representative results are shown.

to perform an additional series of *in vitro* translation experiments specifically designed to study the mechanism(s) of translation repression by HuR, focusing on the 149 nt fragment (890–1038) at the 3′ end of the IGF-IR 5′-UTR. This fragment contains all of the high-affinity HuR binding sites, and these are all located more than 55 nt away from the 5′ end of the RNA (owing in part to the presence of a 42 nt leader generated from the vector sequence). Thus this RNA template maintains the cap-distal nature of the HuR binding sites seen in the intact 5′-UTR. Importantly, we have determined that the IGF-IR internal ribosome entry window is also contained within this fragment, and that this sequence can mediate cap-independent translation initiation relatively efficiently *in vitro*, while the full length IGF-IR 5′-UTR does not (Figure 9A). Therefore, the IGFIR(890–1038)-FLuc reporter RNA successfully recapitulates both the cap-dependent and IRES-mediated translation-initiation features associated with the intact IGF-IR 5′-UTR in cells.

For this series of *in vitro* translation experiments, we utilized purified recombinant GST-HuR (instead of *in vitro* translated HuR) to facilitate quantitative functional assessment of HuR–RNA interactions, and capped *Renilla* luciferase RNA was included in all *in vitro* translation reactions as an internal control. UV crosslinking data confirmed that GST-HuR does specifically bind the IGFIR(890–1038)-FLuc reporter RNA, but does not interact with either the control firefly or *Renilla* luciferase RNA (Figure 9B). A sequence-specific and concentration-dependent repression of translation through the 890–1038 fragment of the IGFIR 5′-UTR by GST-HuR was observed (Figure 9C), similar to that seen with the full-length IGF-IR 5′-UTR reporter RNA and *in vitro* translated untagged HuR (Figure 3).

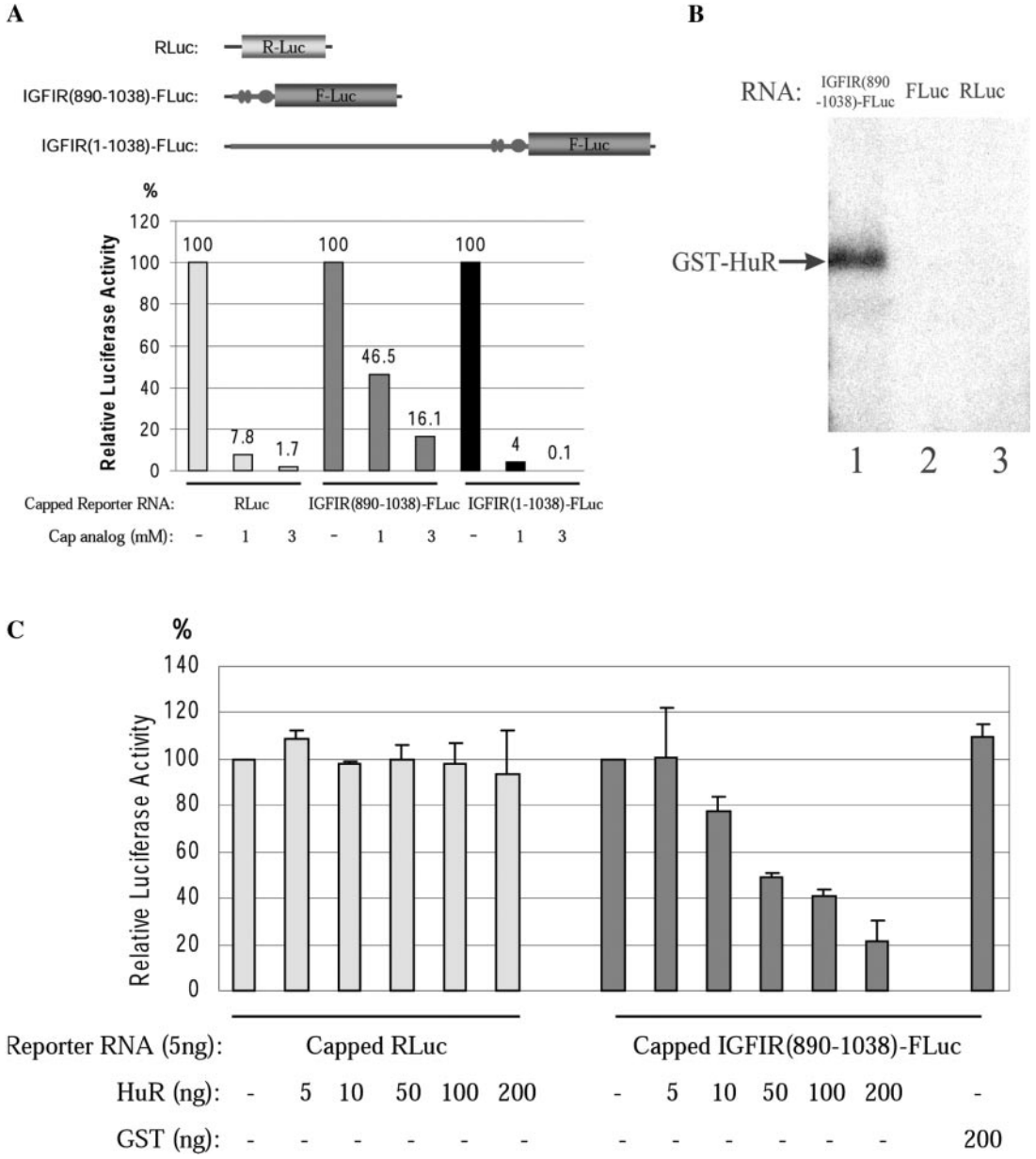

Figure 9. The 890–1038 nt fragment of the IGF-IR 5′-UTR, containing the HuR binding sites and internal ribosome entry window, accurately recapitulates cap-dependent and IRES-mediated translation initiation and HuR repression *in vitro*. (**A**) *In vitro* translation of the control RLuc (*Renilla* luciferase), full-length IGFIR (1–1038)-FLuc, and IGFIR(890–1038)-FLuc reporter RNA (each capped, 5 ng) was performed in the absence or presence of 1 or 3 mM cap analog. Each of the reporter RNAs is diagrammed schematically at the top. The luciferase activities are expressed as a percentage of the control reactions without cap-analog. (**B**) Purified recombinant GST-HuR (62 kDa, 10 ng) was incubated with the [^{32}P]UTP-labeled IGFIR(890–1038)-FLuc, FLuc or RLuc reporter RNAs, and UV crosslinking was performed as described in Materials and Methods. Samples were resolved on 10% SDS–PAGE and visualized by autoradiography. The position of the crosslinked GST-HuR band is indicated by an arrow. (**C**) *In vitro* translation of the IGFIR(890–1038)-FLuc reporter RNA (5 ng) with the internal control RLuc RNA (1 ng) was performed with increasing concentrations of GST-HuR (or GST as a control). The amount of HuR included in each reaction is indicated. The raw data for both the IGFIR(890–1038)-FLuc and the internal control RLuc RNAs are shown. The luciferase activities are expressed relative to the control reaction without GST-HuR. These experiments were repeated at least three times.

Labile repression of cap-dependent translation by HuR

Because the HuR binding sites are positioned upstream of the initiation codon, the translation pre-initiation complex will unavoidably encounter HuR as it linearly scans the 5′ leader sequence. Therefore we speculated that HuR might initially block the progress of the scanning 43S translation pre-initiation complex, but eventually be displaced from its binding sites, resulting in a variability in translational repression over time. As an initial test of this hypothesis, we compared the degree of translation repression by HuR at two time points (10 and 90 min) over a range of HuR concentrations. Consistent with our speculation, we found that the degree of translation repression by HuR changed with time, with a considerably greater degree of repression observed at the earlier time point (Figure 10A).

These results prompted us to perform a more detailed examination of the kinetics of translational repression by HuR. Translation of the reporter RNA in the presence or absence of HuR was monitored at multiple time points (Figure 10B). HuR did not significantly alter synthesis of the internal control *Renilla* luciferase. However, HuR dramatically delayed the translation of the IGFIR(890–1038)-FLuc reporter RNA. A closer inspection of the data revealed that HuR exerts the greatest translation repression at the earliest time points (initially 35-fold repression), decreasing over a relatively short period of time (to 7-fold at 20 min), and reaching a plateau (at ~4–5-fold) thereafter (Figure 10C). This residual translational repression by HuR through the IGF-IR 5′-UTR sequence persisted for at least 90 min.

We were concerned that analysis of cumulative luciferase activities may not accurately discriminate changes in the instantaneous degree of translation repression by HuR, especially at later time points. For example, the apparent late plateau of translational repression observed might have

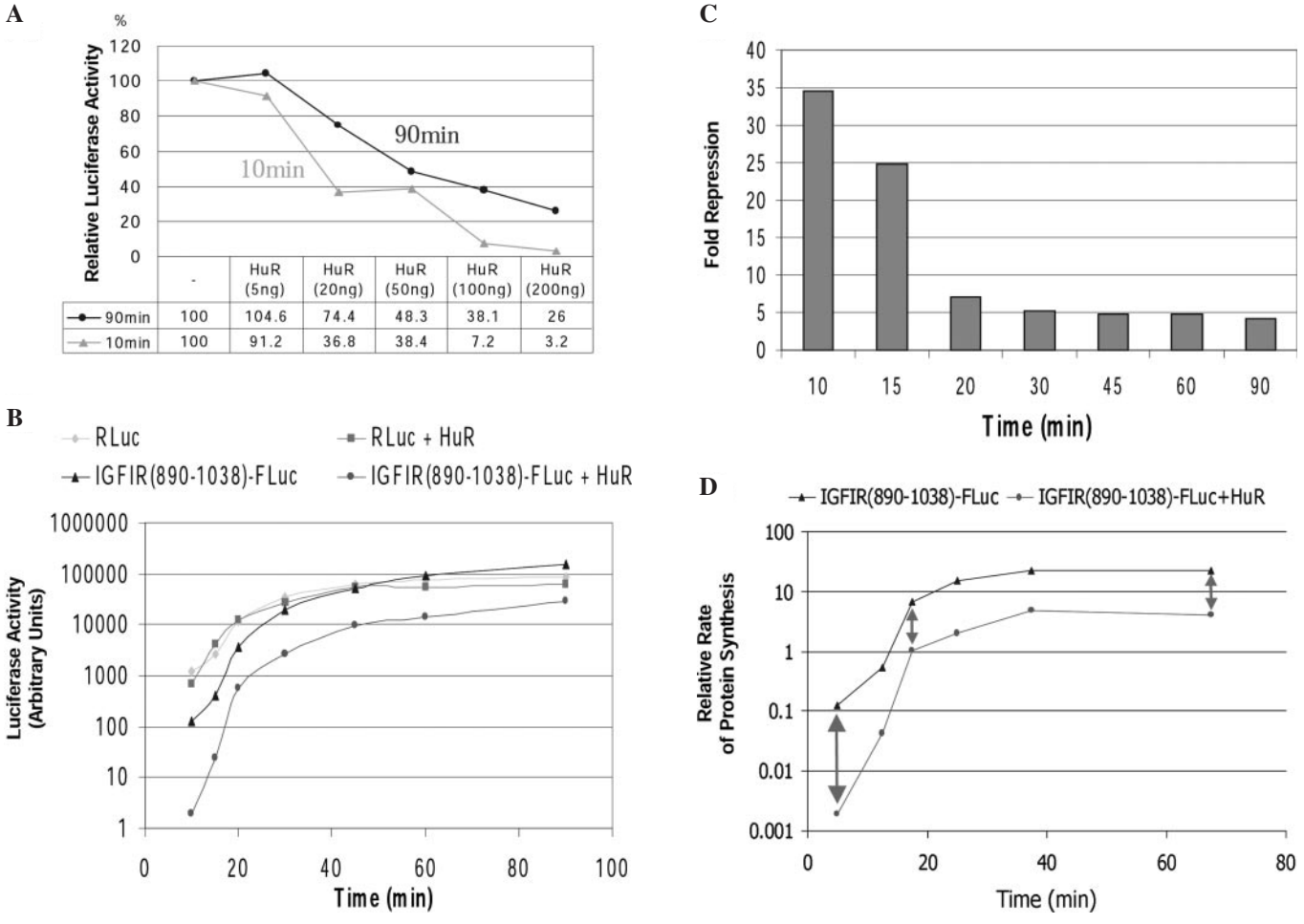

Figure 10. Variability of HuR translational repression over time. (**A**) Standard *in vitro* translation assays were performed using the IGFIR(890–1038)-FLuc reporter RNA and variable concentrations of GST-HuR as indicated. The firefly luciferase activities were normalized using the internal control *Renilla* luciferase RNA. Values obtained using reaction times of 10 or 90 min were compared. The results are expressed as a percentage relative to reactions without HuR, and the numerical data are presented below the graph. (**B**) *In vitro* translation assays were performed using the IGFIR(890–1038)-FLuc RNA (5 ng) and the internal control *Renilla* luciferase RNA (1 ng) with or without GST-HuR (200 ng). The reactions were stopped and luciferase activities measured at 10, 15, 20, 30, 45, 60 and 90 min. The cumulative firefly and *Renilla* luciferase activities in arbitrary units are plotted on a logarithmic scale. (**C**) The data from (B) are expressed as fold repression owing to HuR as a function of time. Firefly luciferase readings were normalized to the internal control *Renilla* luciferase measurements. (**D**) The data from (B) were re-analyzed to assess the relative rate of protein synthesis (change in luciferase activity per unit of time, translation velocity). Calculations were performed as described in Materials and Methods. Data are plotted on a logarithmic scale (arbitrary units), and the degree of translation repression attributable to HuR is represented by the double-headed arrows. The experiment was repeated with essentially identical results.

been produced solely by the initial repression by HuR at the early time points. Therefore, we re-analyzed this data to assess the relative rate of translation (velocity) rather than cumulative protein levels (Figure 10D). The lower rate of translation observed in the presence of HuR is manifested in the vertical distances between the two plots (double-headed arrows). Note that there is initially nearly a two log difference in translation velocity of the IGFIR 5′-UTR reporter RNA with and without HuR. This difference (repression) narrows to less than one log over a short period of time. Importantly, the rate of translation in the presence of HuR never attained the level observed in the absence of HuR.

From these results, there appear to be two phases of translational repression by HuR—an initial phase during which HuR repression is extremely efficient but labile, followed by a secondary phase of lower but relatively constant repression of translational efficiency.

Persistent and potent repression of IRES-mediated translation by HuR

It is important to recognize that the results in Figure 10 reflect a combination of cap-dependent and IRES-mediated translation. The appearance of two phases of HuR translational repression may be indicative of two different mechanisms by which HuR represses translation initiation through the IGF-IR 5′-UTR. In particular, we speculated that HuR might directly interfere with IRES-mediated translation initiation owing to the proximity of its binding sites to the internal ribosome entry window.

To specifically examine the degree and kinetics of HuR repression of IRES-mediated translation, a time-course assay was performed similar to that shown in Figure 10B, except that cap analog was included to specifically block cap-dependent initiation (59–61). HuR very potently repressed translation initiation through the IGF-IR IRES (>97%), and this potent repression remained essentially constant over at least 90 min (Figure 11).

Together, the results presented in Figures 10 and 11 indicate that there are probably two distinct components of HuR translational repression. One of these appears to be kinetically labile (repression of cap-dependent scanning), whereas the other component (repression of IRES-mediated translation initiation) remains static. The combination of these two components can explain the characteristics of HuR translation repression we have observed.

HuR is actively displaced by the scanning ribosome complex, but perpetually arrests internal ribosome entry

To further investigate the two components of translation repression by HuR through the IGF-IR 5′-UTR, quantitative UV crosslinking assays were performed in the presence of RRL, allowing us to directly assess the interactions between HuR and the IGF-IR 5′-UTR RNA in an active *in vitro* translation environment. We had hypothesized that the variability of HuR translational repression over time might be a consequence of dynamic interactions with the 43S scanning ribosome complex.

The results revealed that binding of HuR to the IGF-IR 5′-UTR significantly diminished within 15 min, under conditions conducive to *in vitro* translation (Figure 12A, panel a). By 60 min, ~50% dissociation of HuR was observed. Immunoblot analysis reveals no change in total HuR levels in these reactions (data not shown). This decrease in HuR binding to the IGF-IR 5′-UTR directly correlates with the decrease in translational repression by HuR observed over time.

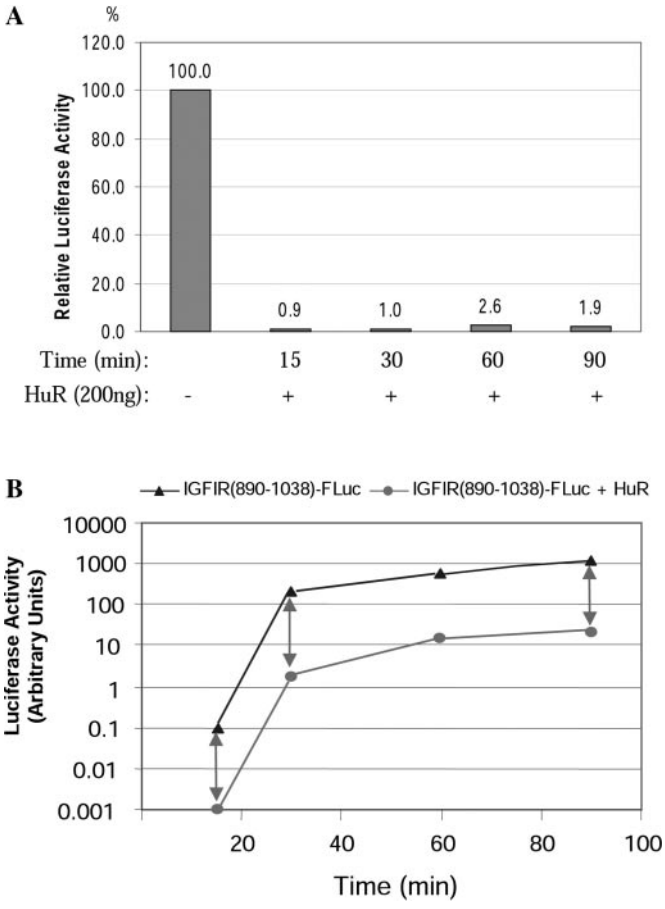

Figure 11. HuR potently and persistently represses IGF-IR IRES-mediated translation initiation *in vitro*. *In vitro* translation assays were performed in the presence of cap analog (3 mM) using the IGFIR(890–1038)-FLuc reporter RNA (5 ng) with or without GST-HuR (200 ng). Individual translation reactions were stopped at various time points as indicated and the luciferase activities were measured. (**A**) The luciferase activities of samples with HuR are expressed relative to those of paired control samples without HuR at each corresponding time point. (For clarity, the paired control samples = 100% for each time point are not shown.) (**B**) Cumulative protein synthesis over time is assessed. Note that a two log decrease in efficiency of IRES-mediated translation in the presence of HuR is maintained throughout the course of the experiment.

In contrast, no decrease in HuR–RNA interaction was observed with inclusion of cap analog in the RRL (panel b). These results suggest that active scanning by the cap-dependent 43S complex is required to actively dissociate HuR from its binding sites. Equally important, these results also indicate that attempted IRES-mediated translation initiation is not capable of displacing HuR, thus accounting for the continuous block of IRES activity observed.

Interestingly, if heparin was added following the *in vitro* translation period, HuR binding was restored (panel c). This indicates that the affinity of HuR for the IGF-IR 5′-UTR sequence is very high (actively binding in the presence of heparin), and by inference, its re-association with the RNA

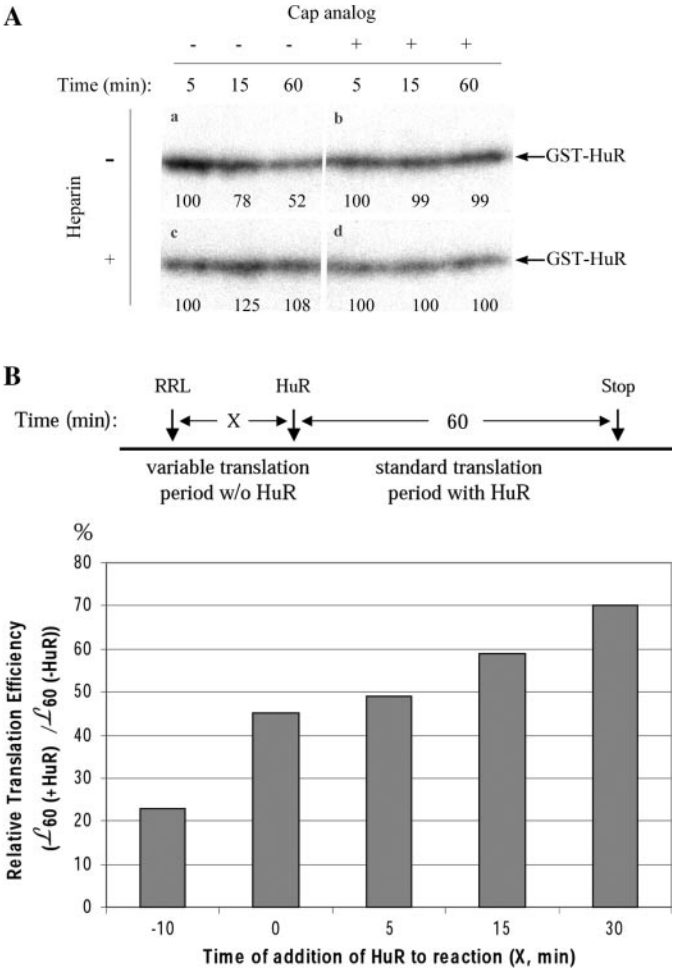

Figure 12. HuR is actively displaced from its binding sites on the IGF-IR 5′-UTR by the cap-dependent scanning 43S ribosome complex but not by IRES-mediated translation initiation, and the effectiveness of HuR as a translational repressor is decreased if it does not occupy its binding sites before commencement of active translation initiation. (**A**) UV crosslinking was utilized to assess HuR binding to the IGF-IR 5′-UTR under conditions conducive to active *in vitro* translation. Standard *in vitro* translation assays were performed using the [^{32}P]-UTP labeled IGFIR(890–1038)-FLuc reporter RNA (5 ng), with GST-HuR (200 ng) included in all samples. Cap analog (3 mM) was included in the samples shown in panels b and d. After *in vitro* translation at 30°C for 5, 15 or 60 min, the samples were immediately transferred to ice. For the samples in panels c and d, heparin (5 mg/ml) was added at this step. Then the samples were exposed to UV irradiation for 30 min on ice, followed by digestion with RNases A and T_1. Equal aliquots of the samples were resolved by SDS–PAGE. The results were obtained by autoradiography. The GST-HuR bands are indicated by arrows. Band intensities were quantified using ScionImage (NIH Image) and expressed (as percentages) relative to the 5 min time point. The experiment was repeated three times and a representative result is shown. (**B**) A two-phase time-course experiment was performed to assess the temporal relationship between HuR RNA-binding and translational repression. The experimental procedure is diagrammed above. An *in vitro* translation reaction using the IGFIR(890–1038)-FLuc reporter RNA (5 ng) was begun at time 0. Following a variable incubation period (X = 0, 5, 15 or 30 min), GST-HuR (200 ng) was added to the reaction, and the incubation continued for an additional standard 60 min period. The luciferase activities attributable to the standard 60 min translation period following HuR addition (L_{60}) were determined by subtracting the luciferase activities attributable to the variable translation period (measured in a series of parallel control samples, L_X) from the total cumulative luciferase activities at time X + 60 (L_{X+60}). The relative translation efficiency in the presence of HuR during the standard 60 min period was compared with that of another set of samples to which HuR was never added. The result [L_{60}(+HuR)/L_{60}(−HuR)] is expressed graphically below. For the sample denoted −10 min, HuR was pre-incubated with the reporter RNA for 10 min prior to addition of RRL.

must have been perpetually blocked by the scanning ribosome complex (in the absence of heparin).

Based on these findings, we would anticipate that the capacity of HuR to function as a site-specific translation repressor would be compromised if active translation preceded its association with the RNA. Indeed, this is the case. If HuR is initially withheld for a variable period of time from the *in vitro* translation reaction, its ability to repress translation over a subsequent standard period of time is progressively diminished (Figure 12B). Thus it appears that the effectiveness of HuR as a repressor of translation initiation is heavily dependent upon occupation of its binding sites before commencement of active scanning by the 43S complex through the 5′-UTR. One potential implication of this result is that association of HuR with the IGF-IR 5′-UTR in the nucleus, perhaps co-transcriptionally, may be essential for its regulatory function *in vivo*.

DISCUSSION

Function of HuR as a 5′-UTR-binding protein/translational repressor

We have begun to investigate the molecular mechanisms by which the complex 5′-untranslated RNA sequence of the human IGF-IR transcript and the proteins with which it interacts contribute to the physiological regulation of IGF-IR expression. Here we have shown that the ELAV protein HuR specifically binds the IGF-IR 5′-UTR and differentially represses cap-dependent and IRES-mediated translation initiation.

HuR has been predominantly characterized as a regulatory protein that binds specifically to consensus ARE within 3′-untranslated sequences of multiple genes and enhances mRNA stability (generally resulting in a net increase in gene expression) (42,43,45,62–65). In this context, HuR enhances mRNA stability apparently by competing with other ARE-binding proteins which would otherwise target the mRNA for degradation from the 3′ end (66,67). However, it is topologically and functionally significant, in the case of the IGF-IR mRNA, that HuR is binding upstream of the initiation codon. Binding of HuR directly to the 5′-UTR of the IGF-IR transcript provides the opportunity for the translation apparatus to encounter this regulatory protein before initiation of translation of the IGF-IR coding sequence. Thus it is reasonable to anticipate a role for HuR in regulation of translation efficiency in the context of its binding the complex IGF-IR 5′-UTR. Indeed, we have consistently observed that binding of HuR to its target sequences within the IGF-IR 5′-UTR was associated with a decrease in translational efficiency both *in vitro* and *in vivo*.

A model for differential repression of cap-dependent versus IRES-mediated translation initiation by HuR

Our functional data are indicative of the existence of two distinct mechanisms of action for HuR in its control of translation initiation through the IGF-IR 5′-UTR (see the model proposed in Figure 13).

First, it appears that HuR significantly delays cap-dependent scanning by the 43S pre-initiation complex (Figure 13, section I). Evidence for this conclusion is observed not only with the 5′-UTR fragment used in the kinetic assays

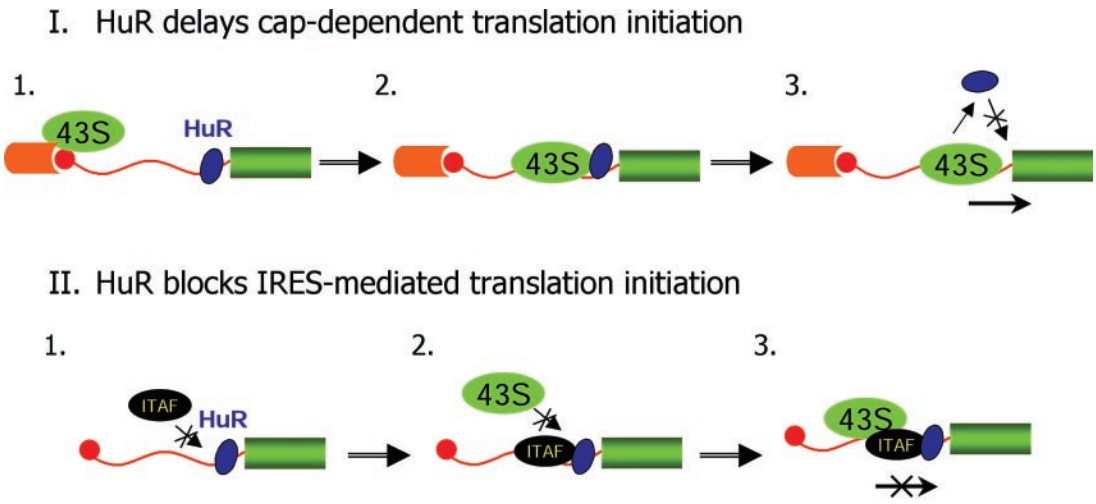

Figure 13. A two-component model for HuR translation repression through the IGF-IR 5′-UTR. The top section depicts the mechanism through which HuR delays translation initiation by the cap-dependent 43S scanning ribosome complex. In Step 1, HuR (blue oval) binds the IGF-IR 5′-UTR, just upstream of the coding sequence (green rectangle). This does not prevent the recruitment of the 43S translation pre-initiation complex (green ellipse) to the cap structure (red circle) through interaction with the eIF4F complex (orange cylinder). In Step 2, the progress of the scanning 43S complex is impeded as a consequence of HuR binding to the 5′-UTR. In Step 3, after a pause, the scanning 43S complex actively displaces HuR from its binding sites, and proceeds to productive translation initiation. It appears that, once HuR is displaced, active scanning of the 5′-UTR perpetually interferes with re-association of HuR with the IGF-IR RNA. The bottom section illustrates three steps at which HuR could block IRES-mediated translation initiation. In Step 1, HuR may interfere with the initial binding of ITAFs to the 5′-UTR. In Step 2, HuR may permit the association of ITAFs with the 5′-UTR, but prevent the ITAFs from recruiting the 43S ribosome complex. In Step 3, HuR may allow formation of the full IRES-associated pre-initiation complex, but block productive translation initiation. We suspect that either Step 2 or 3 is the critical point at which HuR blocks IRES function, because the arrested partial or complete IRES-associated complex, not HuR alone, apparently then becomes resistant to displacement by the cap-dependent scanning ribosome complex.

(Figure 10A and B), but also with the full-length IGF-IR 5′-UTR reporter RNA (Figure 3), where the HuR binding sites are located >890 nt from the 5′ end. Work done with the IRP-IRE system has provided precedent for ribosomal pausing and scanning arrest as a mechanism of translational repression from a cap-distal position (38). Yet, it appears that the scanning translation pre-initiation complex eventually is able to displace HuR from its binding sites (Figure 12A, panel a), accounting for the decline in translation repression at later time points (Figure 10C). Although it is clear that HuR is displaced from its binding site within the IGF-IR 5′-UTR under conditions conducive to ribosomal scanning, we have not formally proven that the scanning 43S ribosomal complex directly displaces HuR; it remains plausible that one or more intermediate steps or factors are involved in mediating this outcome. Nevertheless, once HuR has been actively displaced, it appears that resumption of ribosomal scanning and active translation initiation perpetually interfere with the re-association of HuR with the RNA [Figure 12A (panel c) and B].

Considering the relatively short half-life of mRNA in cells (68), the substantial delay to cap-dependent scanning by HuR is likely to result in a physiologically significant degree of translational repression. The high affinity of HuR for its binding sites within the IGF-IR 5′-UTR may be a contributing factor to this repression. It is also possible that alterations in 5′-UTR RNA structure induced or stabilized by interaction with HuR could influence the processivity of the scanning ribosomal complex [also see (69,70)]. Furthermore, it is reasonable to speculate that, *in vivo*, there may be accessory proteins [translational co-repressors (71,72)] which cooperate with HuR to modulate translational efficiency.

It also appears that HuR is capable of effectively blocking IRES-mediated translation initiation (Figure 13, section II). It is conceivable that HuR could prevent initial association of the IRES *trans*-acting factors (ITAFs) with the RNA (Step 1). Alternatively, HuR could block assembly of the IRES-associated ribosome–ITAF complex at an intermediate stage (Step 2). Finally, HuR may allow the full assembly of the IRES-associated ribosome–ITAF complex, but block its ability to initiate translation (Step 3). We favor either of the two latter possibilities (arrested partial or complete IRES complex) over the first (HuR alone bound to RNA), because it appears that an arrested HuR/ITAF ± ribosome complex must be formed which is resistant to dissociation by cap-dependent 43S scanning complexes (HuR alone would be displaced), accounting at least in part for the plateau in HuR repression (Figure 10B–D) and the residual binding of HuR to the RNA at later time points (Figure 12A). Sequestration of an arrested IRES complex by HuR could explain the highly potent and persistent repression of IRES-mediated translation initiation observed (Figure 11).

The mechanisms of cellular IRES-mediated translation initiation are not well understood (73). A number of positive regulatory proteins enhancing IRES activity have been characterized [including hnRNP C, La, PTB and unr (34,74,75)], and some of these positive ITAFs appear to function as RNA chaperones to facilitate the formation of RNA secondary structure permissive for recruitment of the 40S ribosome subunit (34,35). HuR is one of only a few recognized negative regulators of IRES function [also see (76)]. It is possible that HuR may function as a negative ITAF, not necessarily by blocking binding of positive ITAFs and/or the 40S ribosome subunit, but by locking the 5′-UTR RNA

into a conformation which is not permissive for IRES-mediated translation initiation.

Perspective: the function of HuR in the composite regulation of IGF-IR expression through its complex 5′-UTR

Based on the location of its binding sites, and its function as a dual-purpose translation repressor, HuR is poised to serve as a critical regulator of IGF-IR expression at the translational level. Binding to the extreme 3′ end of the 5′-UTR, just upstream of the translation initiation codon, HuR stands as potentially the final obstacle to translation initiation via the conventional scanning 43S ribosome complex. Furthermore, because IRES-mediated translation initiation is likely to serve as an alternative to cap-dependent scanning under certain physiological conditions, the ability of the cell to modulate HuR's potent repression of the IGF-IR IRES will be crucial to allow appropriate fluctuations in IGF-IR expression in response to changes in microenvironment or cell status.

HuR also binds the 575 nt 5′-UTR of the $p27^{kip1}$ mRNA (77) and functions as a translation repressor in this context as well (46). However, this leaves us with an interesting question regarding the function of HuR in potentially simultaneously inhibiting expression of both a cell-cycle inhibitor and a powerful proliferation enhancer. This apparent contradiction in HuR function could be explained if the ability of HuR to bind its target sequences and repress translation is differentially regulated as a consequence of the distinct architectural organization of these two complex 5′-untranslated RNA sequences. Giraud *et al*. (58) identified PTB as a factor which specifically binds the rat IGF-IR 5′-UTR, and our investigations have yielded evidence for additional regulatory components which can influence the interaction of HuR with its target sites within the human IGF-IR 5′-UTR. We propose that HuR, in concert with these other sequence-specific regulatory proteins and structural features operating through the complex 5′-UTR, combine to provide gene-specific regulation of IGF-IR expression at the translational level.

ACKNOWLEDGEMENTS

We thank Dr Joan A. Steitz (HHMI, Yale University) for kindly providing the pcDNA3-HuR plasmid. We also thank Dr Xiaoyong Yang for helpful discussions, and Dr Greg Cox (Molecular Probes) and Dr Larry Gartland for help with fluorescent tagging of siRNA and flow cytometric analysis of transfected cells. This work was supported by National Institutes of Health grants CA108886 (S.W.B.) and CA80916 (P.D.E.), the UAB SPORE in Ovarian Cancer (S.W.B.) and the Office of Research and Development, Medical Research Service, Department of Veterans Affairs (P.H.K.). Funding to pay the Open Access publication charges for this article was provided by National Institutes of Health grant CA108886.

Conflict of interest statement. None declared.

REFERENCES

1. Ullrich,A., Gray,A., Tam,A.W., Yang-Feng,T., Tsubokawa,M., Collins,C., Henzel,W., Le Bon,T., Kathuria,S., Chen,E. *et al*. (1986) Insulin-like growth factor I receptor primary structure: comparison with insulin receptor suggests structural determinants that define functional specificity. *EMBO J*., **5**, 2503–2512.
2. LeRoith,D. (2000) Insulin-like growth factor I receptor signaling—overlapping or redundant pathways? *Endocrinology*, **141**, 1287–1288.
3. Valentinis,B., Romano,G., Peruzzi,F., Morrione,A., Prisco,M., Soddu,S., Cristofanelli,B., Sacchi,A. and Baserga,R. (1999) Growth and differentiation signals by the insulin-like growth factor 1 receptor in hemopoietic cells are mediated through different pathways. *J. Biol. Chem*., **274**, 12423–12430.
4. Butler,A.A., Yakar,S., Gewolb,I.H., Karas,M., Okubo,Y. and LeRoith,D. (1998) Insulin-like growth factor-I receptor signal transduction: at the interface between physiology and cell biology. *Comp. Biochem. Physiol. B Biochem. Mol. Biol*., **121**, 19–26.
5. Liu,J.L. and LeRoith,D. (1999) Insulin-like growth factor I is essential for postnatal growth in response to growth hormone. *Endocrinology*, **140**, 5178–5184.
6. Holzenberger,M., Dupont,J., Ducos,B., Leneuve,P., Geloen,A., Even,P.C., Cervera,P. and Le Bouc,Y. (2003) IGF-1 receptor regulates lifespan and resistance to oxidative stress in mice. *Nature*, **421**, 182–187.
7. Sell,C., Dumenil,G., Deveaud,C., Miura,M., Coppola,D., DeAngelis,T., Rubin,R., Efstratiadis,A. and Baserga,R. (1994) Effect of a null mutation of the insulin-like growth factor I receptor gene on growth and transformation of mouse embryo fibroblasts. *Mol. Cell. Biol*., **14**, 3604–3612.
8. Sell,C., Rubini,M., Rubin,R., Liu,J.P., Efstratiadis,A. and Baserga,R. (1993) Simian virus 40 large tumor antigen is unable to transform mouse embryonic fibroblasts lacking type 1 insulin-like growth factor receptor. *Proc. Natl Acad. Sci. USA*, **90**, 11217–11221.
9. Parrizas,M., Saltiel,A.R. and LeRoith,D. (1997) Insulin-like growth factor 1 inhibits apoptosis using the phosphatidylinositol 3′-kinase and mitogen-activated protein kinase pathways. *J. Biol. Chem*., **272**, 154–161.
10. Kulik,G., Klippel,A. and Weber,M.J. (1997) Antiapoptotic signalling by the insulin-like growth factor I receptor, phosphatidylinositol 3-kinase, and Akt. *Mol. Cell. Biol*., **17**, 1595–1606.
11. Thimmaiah,K.N., Easton,J., Huang,S., Veverka,K.A., Germain,G.S., Harwood,F.C. and Houghton,P.J. (2003) Insulin-like growth factor I-mediated protection from rapamycin-induced apoptosis is independent of Ras-Erk1-Erk2 and phosphatidylinositol 3′-kinase-Akt signaling pathways. *Cancer Res*., **63**, 364–374.
12. LeRoith,D. and Roberts,C.T.,Jr (2003) The insulin-like growth factor system and cancer. *Cancer Lett*., **195**, 127–137.
13. Pollak,M.N., Schernhammer,E.S. and Hankinson,S.E. (2004) Insulin-like growth factors and neoplasia. *Nature Rev. Cancer*, **4**, 505–518.
14. Abramovitch,S., Glaser,T., Ouchi,T. and Werner,H. (2003) BRCA1–Sp1 interactions in transcriptional regulation of the IGF-IR gene. *FEBS Lett*., **541**, 149–154.
15. Idelman,G., Glaser,T., Roberts,C.T.,Jr and Werner,H. (2003) WT1-p53 interactions in insulin-like growth factor-I receptor gene regulation. *J. Biol. Chem*., **278**, 3474–3482.
16. Werner,H., Shen-Orr,Z., Rauscher,F.J.,III, Morris,J.F., Roberts,C.T.,Jr and LeRoith,D. (1995) Inhibition of cellular proliferation by the Wilms' tumor suppressor WT1 is associated with suppression of insulin-like growth factor I receptor gene expression. *Mol. Cell. Biol*., **15**, 3516–3522.
17. Werner,H., Rauscher,F.J.,III, Sukhatme,V.P., Drummond,I.A., Roberts,C.T.,Jr and LeRoith,D. (1994) Transcriptional repression of the insulin-like growth factor I receptor (*IGF-I-R*) gene by the tumor suppressor WT1 involves binding to sequences both upstream and downstream of the *IGF-I-R* gene transcription start site. *J. Biol. Chem*., **269**, 12577–12582.
18. Werner,H., Karnieli,E., Rauscher,F.J. and LeRoith,D. (1996) Wild-type and mutant p53 differentially regulate transcription of the insulin-like growth factor I receptor gene. *Proc. Natl Acad. Sci. USA*, **93**, 8318–8323.
19. Nair,P.N., De Armond,D.T., Adamo,M.L., Strodel,W.E. and Freeman,J.W. (2001) Aberrant expression and activation of insulin-like growth factor-1 receptor (IGF-1R) are mediated by an induction of IGF-1R promoter activity and stabilization of IGF-1R mRNA and contributes to growth factor independence and increased survival of the pancreatic cancer cell line MIA PaCa-2. *Oncogene*, **20**, 8203–8214.
20. Vecchione,A., Marchese,A., Henry,P., Rotin,D. and Morrione,A. (2003) The Grb10/Nedd4 complex regulates ligand-induced ubiquitination

and stability of the insulin-like growth factor I receptor. *Mol. Cell. Biol.*, **23**, 3363–3372.
21. Cooke,D.W. and Casella,S.J. (1994) The 5′-untranslated region of the IGF-I receptor gene modulates reporter gene expression by both pre- and post-transcriptional mechanisms. *Mol. Cell. Endocrinol.*, **101**, 77–84.
22. Mikulits,W., Pradet-Balade,B., Habermann,B., Beug,H., Garcia-Sanz,J.A. and Mullner,E.W. (2000) Isolation of translationally controlled mRNAs by differential screening. *FASEB J.*, **14**, 1641–1652.
23. Cooke,D.W., Bankert,L.A., Roberts,C.T.,Jr, LeRoith,D. and Casella,S.J. (1991) Analysis of the human type I insulin-like growth factor receptor promoter region. *Biochem. Biophys. Res. Commun.*, **177**, 1113–1120.
24. Mamula,P.W. and Goldfine,I.D. (1992) Cloning and characterization of the human insulin-like growth factor-I receptor gene 5′-flanking region. *DNA Cell Biol.*, **11**, 43–50.
25. Kozak,M. (1987) An analysis of 5′-noncoding sequences from 699 vertebrate messenger RNAs. *Nucleic Acids Res.*, **15**, 8125–8148.
26. van der Velden,A.W. and Thomas,A.A. (1999) The role of the 5′ untranslated region of an mRNA in translation regulation during development. *Int. J. Biochem. Cell Biol.*, **31**, 87–106.
27. Gu,W. and Hecht,N. (1996) Translation of a testis-specific Cu/Zn superoxide dismutase (SOD-1) mRNA is regulated by a 65-kilodalton protein which binds to its 5′ untranslated region. *Mol. Cell. Biol*, **16**, 4535–4543.
28. Nielsen,J., Christiansen,J., Lykke-Andersen,J., Johnsen,A.H., Wewer,U.M. and Nielsen,F.C. (1999) A family of insulin-like growth factor II mRNA-binding proteins represses translation in late development. *Mol. Cell. Biol.*, **19**, 1262–1270.
29. Bag,J. (2001) Feedback inhibition of poly(A)-binding protein mRNA translation. A possible mechanism of translation arrest by stalled 40S ribosomal subunits. *J. Biol. Chem.*, **276**, 47352–47360.
30. Saunders,C. and Cohen,R.S. (1999) The role of oocyte transcription, the 5′UTR, and translation repression and derepression in *Drosophila* gurken mRNA and protein localization. *Mol. Cell*, **3**, 43–54.
31. Niessing,D., Blanke,S. and Jackle,H. (2002) Bicoid associates with the 5′-cap-bound complex of caudal mRNA and represses translation. *Genes Dev.*, **16**, 2576–2582.
32. Miller,S.J., Suthiphongchai,T., Zambetti,G.P. and Ewen,M.E. (2000) p53 binds selectively to the 5′ untranslated region of cdk4, an RNA element necessary and sufficient for transforming growth factor beta- and p53-mediated translational inhibition of cdk4. *Mol. Cell. Biol.*, **20**, 8420–8431.
33. Gray,N.K. and Wickens,M. (1998) Control of translation initiation in animals. *Annu. Rev. Cell Dev. Biol.*, **14**, 399–458.
34. Mitchell,S.A., Spriggs,K.A., Coldwell,M.J., Jackson,R.J. and Willis,A.E. (2003) The Apaf-1 internal ribosome entry segment attains the correct structural conformation for function via interactions with PTB and unr. *Mol. Cell*, **11**, 757–771.
35. Pilipenko,E.V., Pestova,T.V., Kolupaeva,V.G., Khitrina,E.V., Poperechnaya,A.N., Agol,V.I. and Hellen,C.U. (2000) A cell cycle-dependent protein serves as a template-specific translation initiation factor. *Genes Dev.*, **14**, 2028–2045.
36. Galy,B., Creancier,L., Prado-Lourenco,L., Prats,A.C. and Prats,H. (2001) p53 directs conformational change and translation initiation blockade of human fibroblast growth factor 2 mRNA. *Oncogene*, **20**, 4613–4620.
37. Goossen,B. and Hentze,M.W. (1992) Position is the critical determinant for function of iron-responsive elements as translational regulators. *Mol. Cell. Biol.*, **12**, 1959–1966.
38. Paraskeva,E., Gray,N.K., Schlager,B., Wehr,K. and Hentze,M.W. (1999) Ribosomal pausing and scanning arrest as mechanisms of translational regulation from cap-distal iron-responsive elements. *Mol. Cell. Biol.*, **19**, 807–816.
39. Gray,N.K. and Hentze,M.W. (1994) Iron regulatory protein prevents binding of the 43S translation pre-initiation complex to ferritin and eALAS mRNAs. *EMBO J.*, **13**, 3882–3891.
40. Koloteva,N., Muller,P.P. and McCarthy,J.E. (1997) The position dependence of translational regulation via RNA–RNA and RNA–protein interactions in the 5′-untranslated region of eukaryotic mRNA is a function of the thermodynamic competence of 40S ribosomes in translational initiation. *J. Biol. Chem.*, **272**, 16531–16539.
41. Meng,Z., Snyder,R.C., Shrestha,K., Miller,D.M., Emanuel,P.D. and Blume,S.W. (2003) Evidence for differential ribonucleoprotein complex assembly *in vitro* on the 5′-untranslated region of the human IGF-IR transcript. *Mol. Cell. Endocrinol.*, **200**, 127–140.
42. Peng,S.S., Chen,C.Y., Xu,N. and Shyu,A.B. (1998) RNA stabilization by the AU-rich element binding protein, HuR, an ELAV protein. *EMBO J.*, **17**, 3461–3470.
43. Fan,X.C. and Steitz,J.A. (1998) Overexpression of HuR, a nuclear-cytoplasmic shuttling protein, increases the *in vivo* stability of ARE-containing mRNAs. *EMBO J.*, **17**, 3448–3460.
44. Ma,W.J., Cheng,S., Campbell,C., Wright,A. and Furneaux,H. (1996) Cloning and characterization of HuR, a ubiquitously expressed Elav-like protein. *J. Biol. Chem.*, **271**, 8144–8151.
45. Yaman,I., Fernandez,J., Sarkar,B., Schneider,R.J., Snider,M.D., Nagy,L.E. and Hatzoglou,M. (2002) Nutritional control of mRNA stability is mediated by a conserved AU-rich element that binds the cytoplasmic shuttling protein HuR. *J. Biol. Chem.*, **277**, 41539–41546.
46. Kullmann,M., Gopfert,U., Siewe,B. and Hengst,L. (2002) ELAV/Hu proteins inhibit p27 translation via an IRES element in the p27 5′UTR. *Genes Dev.*, **16**, 3087–3099.
47. Mazan-Mamczarz,K., Galban,S., Lopez de Silanes,I., Martindale,J.L., Atasoy,U., Keene,J.D. and Gorospe,M. (2003) RNA-binding protein HuR enhances p53 translation in response to ultraviolet light irradiation. *Proc. Natl Acad. Sci. USA*, **100**, 8354–8359.
48. Nabors,L.B., Gillespie,G.Y., Harkins,L. and King,P.H. (2001) HuR, a RNA stability factor, is expressed in malignant brain tumors and binds to adenine- and uridine-rich elements within the 3′ untranslated regions of cytokine and angiogenic factor mRNAs. *Cancer Res.*, **61**, 2154–2161.
49. Meng,Z., Snyder,R.C., Shrestha,K., Miller,D.M., Emanuel,P.D. and Blume,S.W. (2003) Evidence for differential ribonucleoprotein complex assembly *in vitro* on the 5′-untranslated region of the human IGF-IR transcript. *Mol. Cell Endocrinol.*, **200**, 127–140.
50. Lopez,M.F., Berggren,K., Chernokalskaya,E., Lazarev,A., Robinson,M. and Patton,W.F. (2000) A comparison of silver stain and SYPRO Ruby Protein Gel Stain with respect to protein detection in two-dimensional gels and identification by peptide mass profiling. *Electrophoresis*, **21**, 3673–3683.
51. Gharahdaghi,F., Weinberg,C.R., Meagher,D.A., Imai,B.S. and Mische,S.M. (1999) Mass spectrometric identification of proteins from silver-stained polyacrylamide gel: a method for the removal of silver ions to enhance sensitivity. *Electrophoresis*, **20**, 601–605.
52. Robinow,S., Campos,A.R., Yao,K.M. and White,K. (1988) The elav gene product of *Drosophila*, required in neurons, has three RNP consensus motifs. *Science*, **242**, 1570–1572.
53. Burd,C.G. and Dreyfuss,G. (1994) Conserved structures and diversity of functions of RNA-binding proteins. *Science*, **265**, 615–621.
54. Fan,X.C. and Steitz,J.A. (1998) HNS, a nuclear-cytoplasmic shuttling sequence in HuR. *Proc. Natl Acad. Sci. USA*, **95**, 15293–15298.
55. Pinol-Roma,S., Choi,Y.D., Matunis,M.J. and Dreyfuss,G. (1988) Immunopurification of heterogeneous nuclear ribonucleoprotein particles reveals an assortment of RNA-binding proteins. *Genes Dev.*, **2**, 215–227.
56. Chen,C.Y., Xu,N. and Shyu,A.B. (2002) Highly selective actions of HuR in antagonizing AU-rich element-mediated mRNA destabilization. *Mol. Cell. Biol.*, **22**, 7268–7278.
57. Ostareck-Lederer,A., Ostareck,D.H., Standart,N. and Thiele,B.J. (1994) Translation of 15-lipoxygenase mRNA is inhibited by a protein that binds to a repeated sequence in the 3′ untranslated region. *EMBO J.*, **13**, 1476–1481.
58. Giraud,S., Greco,A., Brink,M., Diaz,J.J. and Delafontaine,P. (2001) Translation initiation of the insulin-like growth factor I receptor mRNA is mediated by an internal ribosome entry site. *J. Biol. Chem.*, **276**, 5668–5675.
59. Ostareck,D.H., Ostareck-Lederer,A., Wilm,M., Thiele,B.J., Mann,M. and Hentze,M.W. (1997) mRNA silencing in erythroid differentiation: hnRNP K and hnRNP E1 regulate 15-lipoxygenase translation from the 3′ end. *Cell*, **89**, 597–606.
60. Grobe,K. and Esko,J.D. (2002) Regulated translation of heparan sulfate *N*-acetylglucosamine *N*-deacetylase/*N*-sulfotransferase isozymes by structured 5′-untranslated regions and internal ribosome entry sites. *J. Biol. Chem.*, **277**, 30699–30706.

61. Nekrasov,M.P., Ivshina,M.P., Chernov,K.G., Kovrigina,E.A., Evdokimova,V.M., Thomas,A.A., Hershey,J.W. and Ovchinnikov,L.P. (2003) The mRNA-binding protein YB-1 (p50) prevents association of the eukaryotic initiation factor eIF4G with mRNA and inhibits protein synthesis at the initiation stage. *J. Biol. Chem.*, **278**, 13936–13943.
62. Brennan,C.M. and Steitz,J.A. (2001) HuR and mRNA stability. *Cell Mol. Life Sci.*, **58**, 266–277.
63. Wang,W., Furneaux,H., Cheng,H., Caldwell,M.C., Hutter,D., Liu,Y., Holbrook,N. and Gorospe,M. (2000) HuR regulates p21 mRNA stabilization by UV light. *Mol. Cell. Biol.*, **20**, 760–769.
64. Wang,W., Caldwell,M.C., Lin,S., Furneaux,H. and Gorospe,M. (2000) HuR regulates cyclin A and cyclin B1 mRNA stability during cell proliferation. *EMBO J.*, **19**, 2340–2350.
65. Nabors,L.B., Suswam,E., Huang,Y., Yang,X., Johnson,M.J. and King,P.H. (2003) Tumor necrosis factor alpha induces angiogenic factor up-regulation in malignant glioma cells: a role for RNA stabilization and HuR. *Cancer Res.*, **63**, 4181–4187.
66. Chen,C.Y., Gherzi,R., Ong,S.E., Chan,E.L., Raijmakers,R., Pruijn,G.J., Stoecklin,G., Moroni,C., Mann,M. and Karin,M. (2001) AU binding proteins recruit the exosome to degrade ARE-containing mRNAs. *Cell*, **107**, 451–464.
67. Brewer,G. (1999) Evidence for a 3′–5′ decay pathway for c-myc mRNA in mammalian cells. *J. Biol. Chem.*, **274**, 16174–16179.
68. Ross,J. (1995) mRNA stability in mammalian cells. *Microbiol. Rev.*, **59**, 423–450.
69. Fouts,D.E., True,H.L. and Celander,D.W. (1997) Functional recognition of fragmented operator sites by R17/MS2 coat protein, a translational repressor. *Nucleic Acids Res.*, **25**, 4464–4473.
70. Schlax,P.J., Xavier,K.A., Gluick,T.C. and Draper,D.E. (2001) Translational repression of the *Escherichia coli* alpha operon mRNA: importance of an mRNA conformational switch and a ternary entrapment complex. *J. Biol. Chem.*, **276**, 38494–38501.
71. Sonoda,J. and Wharton,R.P. (2001) *Drosophila* brain tumor is a translational repressor. *Genes Dev.*, **15**, 762–773.
72. Grskovic,M., Hentze,M.W. and Gebauer,F. (2003) A co-repressor assembly nucleated by sex-lethal in the 3′UTR mediates translational control of *Drosophila* msl-2 mRNA. *EMBO J.*, **22**, 5571–5581.
73. Hellen,C.U. and Sarnow,P. (2001) Internal ribosome entry sites in eukaryotic mRNA molecules. *Genes Dev.*, **15**, 1593–1612.
74. Kim,Y.K., Back,S.H., Rho,J., Lee,S.H. and Jang,S.K. (2001) La autoantigen enhances translation of BiP mRNA. *Nucleic Acids Res.*, **29**, 5009–5016.
75. Kim,J.H., Paek,K.Y., Choi,K., Kim,T.D., Hahm,B., Kim,K.T. and Jang,S.K. (2003) Heterogeneous nuclear ribonucleoprotein C modulates translation of c-myc mRNA in a cell cycle phase-dependent manner. *Mol. Cell. Biol.*, **23**, 708–720.
76. Kim,Y.K., Hahm,B. and Jang,S.K. (2000) Polypyrimidine tract-binding protein inhibits translation of bip mRNA. *J. Mol. Biol.*, **304**, 119–133.
77. Millard,S.S., Vidal,A., Markus,M. and Koff,A. (2000) A U-rich element in the 5′ untranslated region is necessary for the translation of p27 mRNA. *Mol. Cell. Biol.*, **20**, 5947–5959.